

1 Simulation modelling and analysis of linkage-controlled traffic scheme in
2 waterway transport key nodes

3 Yang Liu ^{a, b}, Jingxian Liu ^{a, b, c}, Yi Liu ^{a, b, c, *}, Qian Zhang ^d, Jingwen Shu ^a, Yijun Zhang ^e

4 ^a (*School of Navigation, Wuhan University of Technology, 430063, China*)

5 ^b (*State Key Laboratory of Maritime Technology and Safety, Wuhan University of
6 Technology, Wuhan, 430063, China*)

7 ^c (*National Engineering Research Center for Water Transport Safety, Wuhan University of
8 Technology, 430063, China*)

9 ^d (*School of Engineering, Liverpool John Moores University, Liverpool, L3 3AF, UK*)

10 ^e (*Chang Jiang River Administration of Navigational Affairs, Wuhan, 420100, China*)

11 Abstract: As global shipping undergoes rapid expansion, pivotal waterway transport systems—
12 including significant nodes like the Panama Canal, the Suez Canal, and the Three Gorges-Gezhouba
13 dams—are increasingly emerging as system-wide bottlenecks that limit transportation capabilities.
14 Recognizing the pressing need for efficient traffic organization at these critical junctures, we
15 designed a hybrid simulation model, which integrates Cellular Automaton and Multi-Agent methods,
16 to analyse traffic efficiency and evaluate different ship organization schemes at these key waterway
17 nodes. The Three Gorges-Gezhouba dams serve as a case study, where we crafted and executed four
18 simulation scenarios that accommodate a range of variables such as different traffic organization
19 schemes, traffic flow volumes, and anchorage capacities. Key operational indicators such as the
20 maximum average waiting time of ships at the anchorage, and the period when the anchorage along
21 the waterway reaches saturation, provide insights into the system's operational condition. The
22 simulation outcomes highlight the proposed model's capability to accurately quantify the impact of
23 implementing a linkage-control scheme and underscore the utility of dynamic adjustment of water
24 area ranges under linkage-control for managing various traffic scenarios. Consequently, our research
25 not only enriches high-precision simulation methodologies but also bolsters decision-making
26 processes concerning ship traffic organization at waterway transport key nodes.

27 Keywords: Ship traffic organisation; Cellular automaton; Multi-agent; Waterway transport key
28 nodes; Linkage control

29 Yi Liu

30 liyihy@whut.edu.cn

31 +86 18671456196

32 1178 Youyi Avenue, Wuchang District, Wuhan City, Hubei Province, China

33 1. Introduction

34 In Global shipping, waterway transport key nodes (WTKNs) such as the Panama Canal, Suez
35 Canal, Strait of Malacca, and the Three Gorges-Gezhouba dams (TGGD) hold significant strategic
36 and economic value due to their unique geographical positioning. In the wake of the cessation of
37 the COVID-19 pandemic and the accompanying resurgence of the global economy, maritime trade
38 worldwide is undergoing swift expansion.

39 Due to the surge in transport demand, the Panama Canal has experienced congestion, and the
40 average waiting time for ships has increased from 5 to 6 days to about 10 days, some ships need 9
41 days to pass through the canal, while the usual time is only about 2 days. In 2021, a container ship
42 named “Ever Given”, which was about 400 metres long and weighed about 200,000 tonnes, ran
43 aground in the canal on March 23, blocking the bi-directional traffic of the Suez Canal and leaving
44 more than 300 ships stranded near the canal for more than a week. As China's most substantial water
45 conservancy project, the TGGD face a significant burden of navigation (Liu et al., 2014). The water
46 region surrounding the TGGD has increasingly seen ships pausing their navigation and waiting due
47 to the constraints of the ship locks' carrying capacity (Zhao et al., 2020). WTKNs are experiencing
48 escalating navigational pressures, progressively morphing into chokepoints that curtail traffic
49 efficiency. In light of this context, it has become a great challenge that how to alleviate the
50 accumulation of ship traffic management pressure resulting from the inevitable imbalance of limited
51 navigational resources and growing traffic demands at WTKNs. Despite the criticality of these areas,
52 a paucity of research exists focusing on ship traffic organisation and management in WTKNs. Under
53 such circumstances, applicable method of navigational efficiency and managing performance
54 analysis become paramount.

55 There is a lack of appropriate analytical methods and models for the efficiency of navigational
56 and traffic organisation schemes for complex waterway transport systems. These WTKNs, which
57 are jointly constituted by waterways, anchorages, narrow bottlenecks or ship locks, share the same
58 theoretical problems, but need to be modelled and analysed in a way that is specific to the object of
59 study. To address these issues, we have developed an analytical framework and use simulation
60 methods to simulate and analyse the state of the transport system and the effectiveness of the traffic
61 organisation of the WTKNs. The major contributions of this paper are as follows:

62 (1) The navigational efficiency of ships crossing Waterway Transport Key Nodes (WTKNs) is
63 represented through a robust mathematical model. This model allows for the precise calculation of
64 efficiency indices across various traffic organisation schemes. Additionally, a sophisticated
65 framework has been developed for analysing lock-passing ship traffic organisations. This
66 framework facilitates the detailed calculation and quantification of various levels of saturation and
67 traffic efficiency, enhancing the theoretical understanding of navigable waterways' operational
68 dynamics.

69 (2) A traffic simulation model using Cellular Automaton (CA) and Multi-Agent methods was
70 developed for WTKNs to offer a nuanced analysis of navigation efficiency and ship delay under
71 various anchoring setups. This model intelligently expands anchorages, allowing for a deeper
72 theoretical exploration into how different anchoring configurations affect traffic flow and delay. The
73 integration of CA and multi-agent systems provides a comprehensive tool for simulating and
74 studying complex interactions and dynamics at critical waterway junctions.

75 (3) Experiments adopting several scenarios considering different traffic organisation scheme,
76 traffic volume, and anchorage capacity were formed and conducted using the TGGD as a genuine
77 case for examination. The best anchorage adjustment plan and traffic organisation scheme can be
78 chosen through a comparative examination of the outcomes based on the effectiveness of the
79 navigation.

80 This paper is organised as follows. The pertinent literature on ship traffic organisation and

81 traffic modelling are reviewed in the second section. The third section elaborates on the research
82 object and problem of the traffic behaviour of ship lockage, and the fourth section presents the
83 quantitative analysis and mathematical expression of the traffic behaviour of ships passing through
84 the TGGD water region. The fifth section proposed a method for simulating a multi-node ship traffic
85 system based on CA and multi-agent theories for the water area of large water conservancy hubs.
86 The simulation experiments and discussions are provided in the sixth section, and conclusions and
87 potential directions for further study are covered in the seventh section.

88 **2. Literature Review**

89 The operation of a traffic system heavily depends on traffic organisation. The traffic
90 organisation plan determines how effectively a traffic system operates. There is little research on
91 the organisation of traffic in the WTKNs. The following related areas were included in the literature
92 review:

93 **2.1 Ship traffic organisation methods**

94 Numerous academics have investigated the best ways to organise and regulate traffic in certain
95 water bodies, such as the San Francisco Bay, the Finland Bay, the Istanbul and Singapore Straits,
96 the Bohai Bay, and the Ningbo Zhoushan Waters (Goerlandt et al., 2011, Montewka et al., 2014).
97 Aydogdu et al. (2012.) suggested a management-oriented strategy for organising ship traffic based
98 on a number of research findings on the Istanbul Strait and in accordance with the spatiotemporal
99 distribution features of traffic flow. Wang and Schonfeld (2007) investigated a method for
100 calculating the profit of canal transportation under the conditions of lock closure and service time
101 modification, integrated the demand elasticity into the simulation model, and optimised the
102 transportation. By fusing AHP and TOPSIS, Shi et al. (2019) created a decision-making model to
103 help enhance the lock's carrying capacity, identified the relevant factors, and prioritised them. Li et
104 al. (2020) provided a comprehensive overview of the applications of traffic bottleneck models in
105 traffic management and proposed potential directions for future research in this area, including the
106 consideration of the impact of autonomous driving and communication technologies on traffic flow
107 efficiency. Based on the traffic bottleneck model, Deng et al. (2021) established a method of moving
108 the service time window to manage lock congestion caused by the uneven distribution of ship traffic
109 demands. Liu et al. (2021a, 2021b) proposed a mixed-integer linear programming (MILP) model
110 for integrated planning of berth allocation and ship sequencing in a one-way navigation channel
111 seaport, aiming to minimize the weighted dwelling time of all ships. Ksciuka (2023) et al. reviewed
112 and analysed the uncertainties in maritime transport, finding that uncertainties in port operations are
113 very important for improving the efficiency of transportation. Zhang et al. (2024) explore the ship
114 traffic scheduling problem with uncertain arrival and departure times using a hybrid optimization
115 method. This method combines a memetic algorithm for global exploration with a variable
116 neighbourhood search algorithm, which utilizes problem-specific neighbourhood operators for local
117 search.

118 It has been discovered that most of the research on waterway traffic organisation and
119 performance assessment has focused on the use of optimisation algorithms and management policies,
120 with simulation methods (Zhang et al., 2008) less frequently applied to the organisation of traffic at
121 WTKNs.

122 **2.2 Ship traffic study in WTKNs**

123 A model developed by Ungo et al. (2012) provides an analysis of the competitive dynamics of
124 the shipping routes through the Panama Canal in comparison with alternative routes, using total
125 transport costs as a basis. Muirhead et al. (2015) developed a scenario-based model using Monte
126 Carlo simulation to explore potential shifts in maritime traffic patterns following the expansion of
127 the Panama Canal. Carse (2012) examined the traffic services and management of the Panama Canal

128 from the perspective of infrastructure and environment. Pangano et al. (2016) investigated the
129 economic impact of the canal expansion on Panama's maritime industry cluster. Fan et al. (2022)
130 dissected the blockage incident in the Suez Canal in 2021, underscoring the severe implications of
131 such disruptions in WTKNs. Agussurja et al. (2018) optimised modelling under resource constraints
132 tailored to the specific circumstances of the Strait of Singapore, effectively alleviating navigational
133 pressure by reducing traffic density and ship delay. Qu et al. (2012a) proposes a decision tree model
134 to estimate the loss to global economy on the hypothesis of an extreme scenario of blockade of the
135 Straits of Malacca and Singapore. Zhang et al. (2019) harnessed AIS big data to analyse maritime
136 traffic demand and the spatio-temporal dynamics of ship traffic in the Strait of Singapore. Nofandi
137 et al. (2022) utilised the Vessel Traffic Service (VTS) system Fenix to address ship congestion in
138 the Strait of Malacca and the Strait of Singapore, optimising both traffic safety and efficiency. It
139 can be found that the research on traffic organisation and efficiency assessment methods for
140 WTKNs still needs further improvement.

141 **2.3 Traffic simulation model**

142 Waterway traffic simulation has a long history, and the original models were generally based
143 on rules, queueing model and Arene software, etc. Köse et al. (2003) conducted a simulation of the
144 Istanbul Strait under distinct traffic conditions, analyzing the outcomes and exploring the potential
145 effects of an anticipated rise in marine traffic resulting from new oil pipelines. Mavrakakis et al. (2008)
146 presents a queueing model for maritime traffic in the crowded and challenging Bosphorus Straits,
147 considering its physical characteristics and maritime regulations. Almaz et al. (2012) presents a
148 simulation model for vessel traffic in Delaware River, studied the impact of deepening on
149 navigational efficiency, port performance measures, and risk analysis. Rahimikelarijani et al. (2018)
150 concentrate on simulating and analyzing vessel traffic and operations in the Houston Ship Channel.
151 They employ a discrete event model in Arena to evaluate various closure scenarios using real-world
152 data.

153 The application of CA in transportation first appeared in road traffic and is currently one of the
154 most widely used models. The Wolfram model (e.g., Wolfram et al., 1983, 1984a, 1984b), Nagel–
155 Schrechenberg (NaSch) model (Nagel and Schreckenberg, 1992), BML model (Biham et al., 1992),
156 and other traditional CA traffic flow models are a few examples. Researchers mostly study the
157 effects of slow-start, acceleration, and deceleration, followed by traffic, when using the single-lane
158 model. Ren et al. (2016) constructed a linear motion model to describe the non-uniform bicycle
159 traffic at signalised junctions and examine the impact of the dispersion phenomena on the
160 effectiveness of bicycle passing. By simulating vehicle characteristics and intertemporal distances,
161 Ruan et al. (2017) created a simulation model to precisely compute traffic loads on infrastructure,
162 such as bridges. To demonstrate how a reverse left-turn lane can increase the capacity of
163 intersections to pass through traffic, Chen et al. (2019) built a simulation model that can simulate
164 vehicles turning left at crossings. Sun et al. (2023) built a simulation model based on the driving
165 differences between human-driven cars and self-driving cars, and analysed the impact of trust level
166 on traffic efficiency from two perspectives: efficiency and safety.

167 The CA model has been used extensively in simulations of ship traffic flow. In the original
168 model, the speed of the ship remained constant during voyage, and the speed of each ship in the
169 channel was similar (Liu et al., 2010). After an improvement, the ship's speed in the model is set
170 according to the type of a ship, and it then increases or decreases in accordance with the ship's
171 subsequent behaviour (Blokus et al., 2014). Researchers have incorporated random variables into
172 the automata model in the simulation of ship traffic flow to capture the impact of environmental
173 factors on ship movements (e.g., Qi et al., 2017a, 2017b, Qu et al., 2012b). Studies on the effects of
174 lane switching on traffic efficiency have also been conducted due to the approach channel's
175 increased bustle (e.g. Sun et al., 2015, Hu et al., 2017, Qi et al., 2021).Feng (2013) proposed a model

176 considering channel narrowing near the bridge area and examined the impact of the warning zone's
177 length and ship arrival pattern on the channel's transit capacity.

178 The demand for the precision of ship traffic simulation has likewise increased as computer
179 technology has advanced. The functionality of the simulation model has been further enhanced by
180 the addition of more traffic agents. Similarly, the use of multi-agent simulation technology in the
181 field of transportation is expanding rapidly (e.g., Zhang et al., 2005, Vaněk et al., 2011, 2013).
182 Examples include the MATES model (Fujii et al., 2017) based on a multi-agent framework, the
183 microscopic model of an intersection (Karaaslan et al., 2018), and the model of an urban
184 macroscopic road network (Souza et al., 2019). A simulation model that combines CA and multi-
185 agent systems has been developed. By incorporating a multi-agent structure into a continuous CA
186 model, Yeldan et al. (2012) investigated the impact of driver and vehicle heterogeneity on traffic.
187 Deo et al. (2014) studied the impact of various vehicle types on traffic using one-way single-lane
188 intersection and two-way two-lane T-intersection models. Based on multi-agent technology,
189 Vranken et al. (2021) investigated the impact of the share of autonomous vehicles on road capacity.
190 Zhao et al. (2018) studied intersection conflict and congestion in a scenario with automated driving
191 using a CA model. Małecki (2018) established a mixed traffic model that included roadways and
192 parking lots using CA and multi-agents, and they studied the impact of traffic flow, speed, and trip
193 duration in the research areas on drivers' behaviours. To study the traffic efficiency of road
194 intersections under various traffic strategies, Wang et al. (2021) developed a simulation model based
195 on CA and multi-agents, combining the high efficiency of CA with the capability of multi-agents to
196 simulate complex elements. Zhang et al. (2022) established a model combining discrete event
197 simulation and multi-agent model to study the maximum navigation capacity of the Three Gorges
198 dam under the new traffic organization scheme. Liu et al. (2024) developed a heterogeneous traffic
199 flow simulation model based on CA that coexists autonomous and manned ships.

200 Waterway traffic simulation techniques based on CA and multi-agent systems have also been
201 introduced. Using an agent to define the features and autonomous behaviours of each ship. Jiang et
202 al. (2019) developed a combined CA and multi-agent simulation model based on ship behaviour,
203 which confirmed the significant influence of ship behaviour on port operations. In a similar vein,
204 Liu et al. (2021) employed CA and multi-agent simulation techniques to create a simulation model
205 that emulates the arrival and departure of the Liquefied Natural Gas (LNG) carriers at ports. By
206 comparing various traffic organization schemes, they evaluated the navigation and port operation
207 efficiency of the LNG carriers in the simulation.

208 In summary, it becomes evident that there is a relative scarcity of research concerning the
209 traffic organisation and efficiency evaluation pertaining to WTKNs. Moreover, there is a
210 conspicuous absence of methodologies utilising simulation models from the perspective of ship
211 traffic flow. The accuracy and adaptability of existing methods necessitate further enhancement.

212 **3 Problem statement**

213 **3.1 Presentation of WTKNs**

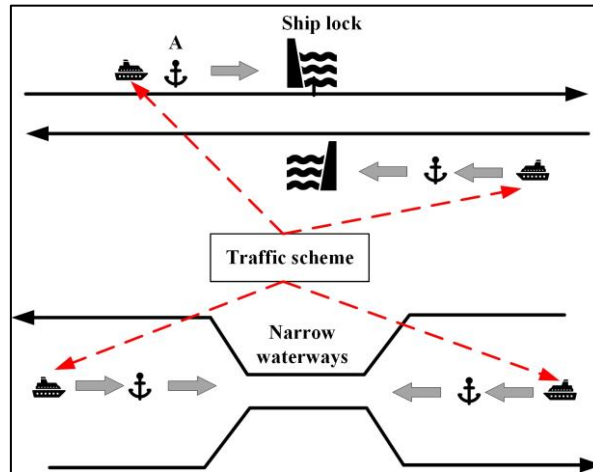
214 WTKNs consist of critical infrastructures that support global or domestic maritime
215 transportation. They primarily encompass the Panama Canal, the Suez Canal, and the TGGD. Each
216 of these structures comprises several key components.

217 Anchorages, for instance, are crucial areas within the WTKNs where ships can safely wait
218 before transiting or while dealing with administrative procedures. The fairways, or navigational
219 channels, are designated routes marked with aids to navigation, allowing safe passage of ships.

220 Ship locks, which play a critical role in these structures, particularly in the Panama Canal and
221 the TGGD, enabling ships to navigate through different water levels by raising or lowering the water
222 level within the lock. They essentially serve as water elevators for ships.

223 Constricted sections or narrow passages in the fairways, such as those found in the Suez Canal
224 and the Strait of Malacca, pose particular navigational challenges, requiring skilled pilots and strict
225 traffic regulation to ensure safety.

226 Finally, each of these components is bound by a complex system of traffic scheme and
227 procedures designed to ensure smooth and efficient transit while maintaining safety and
228 environmental standards. Together, these parts contribute to the unique and vital role that WTKNs
229 play in maritime transport, as shown in Fig. 1.



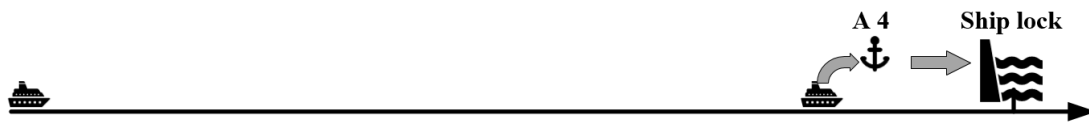
230
231 **Fig. 1.** Structure of WTKNs

232 The carrying capacity of WTKNs is inherently limited by physical constraints. Key among
233 these are narrow passages in the navigational channels and the presence of locks. Narrow passages
234 or constrictions present particular challenges. They require meticulous navigation and often can
235 only accommodate one-way traffic, leading to scheduling constraints and potential delays.
236 Meanwhile, locks, which are used to elevate or lower ships between different water levels, have a
237 limited capacity and necessitate time for filling and emptying, thus creating a bottleneck in the
238 system. When navigational demand outstrips the limited capacity of these key nodes, it results in a
239 backlog of ships, often causing them to anchor and wait their turn for transit. This situation can lead
240 to considerable delays, disrupting shipping schedules and impacting the efficiency of global
241 maritime trade. Therefore, the management and scheme of these constraints is crucial to maintain
242 the fluidity of traffic and minimise waiting times at these vital junctions in the world's maritime
243 network.

244 **3.2 Ship traffic organisation**

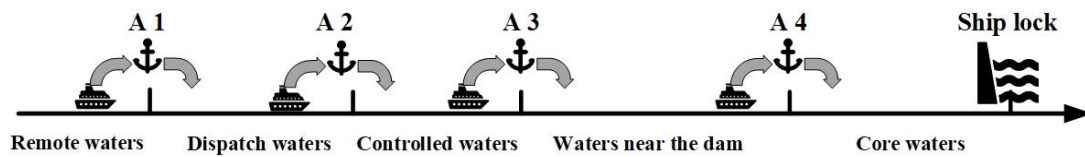
245 For WTKNs, the traffic organisation schemes typically implemented are often relatively
246 straightforward, usually adhering to a first-come-first-served principle. This entails that ships
247 arriving first pass through locks or channel narrows ahead of those arriving later. However, there
248 are also more specialised scheduling methods in place. For instance, the TGGD implemented a
249 linkage control method for ship organisation and scheduling in 2018. What follows is a comparison
250 of ship traffic patterns at the TGGD before and after the introduction of this linked control scheme.

251 Before implementing the linkage control scheme, both upstream and downstream ships must
252 find a place to anchor close to the dam, wait for the ships in front of them to pass, and then line up
253 to enter the ship lock, as shown in **Fig. 2**. However, owing to the rapid development of the Yangtze
254 River shipping industry, there is a high demand for ships to pass through the Three Gorges Dam.
255 Consequently, many ships wait at the anchorage close to the dam because of the limited carrying
256 capacity of the Three Gorges Ship Locks and the high need for ships to pass through the ship lock.
257 The number of ships that need to berth cannot be accommodated by the anchorage capacity.



258
259 **Fig. 2. Schematic of ships passing through a lock.**

260 The linkage control scheme for ships passing the dam has been in effect since 2018 according
261 to the Yangtze River Navigation Administration, as shown in **Fig. 3**. The main goal of the scheme
262 is to arrange these ships in anchorages and waiting areas along the ships' routes in the order and
263 locations specified in the navigation plan submitted to the responsible department by ships passing
264 through the Three Gorges dam and gradually despatch the ships to be locked to the core waters in
265 accordance with the operational efficiency of the Three Gorges dam waterway transportation system.



267
268 **Fig. 3. Schematic of a Ship Passing a Lock after Implementing Linkage Control.**

269 **3.3 The Three Gorges-Gezhouba Dams**

270 Given the complexity and representativeness of the navigation system composed of the TGGD
271 and its upstream and downstream waters, this study addresses the organization and effectiveness of
272 traffic at WTKNs from the perspective of ship traffic flow. Mathematical models were introduced
273 to establish a traffic analysis framework capable of assessing the efficiency of ship traffic and the
274 degree of anchorage saturation.

275 The Yangtze River has developed into the busiest inland river in the world over a long period.
276 According to statistics, more than 3.5 billion tons of cargo was transported via ports along the
277 Yangtze River trunk line in 2021.¹ As the shipping industry of the Yangtze River has grown, the
278 traffic efficiency in the area has deteriorated. Owing to limitations in the carrying capacity of
279 navigation infrastructure, ships in the TGGD water region have become accustomed to stopping and
280 waiting for locks to open in recent years. The TGGD as the transport key node of Yangtze River, its
281 lack of sufficient carrying capacity has limited shipping along the Yangtze River.

282 The main body of the Three Gorges dam is composed of a concrete gravity dam, a flood release
283 gate, a hydropower plant behind an embankment, a permanent fifth-class ship lock, and a ship lift,
284 which are the hub's navigation areas. The other major components are structures associated with
285 power generation and navigation. The Gezhouba dam, which is 38 km downstream of the Three
286 Gorges dam, consists of a ship lock, a power plant, a sluice gate, a scouring sluice, and water-
287 holding structures. A fleet can pass through the 1st and 2nd ship locks with a load between 12000
288 and 16000 tonnes at a time because the locks have an effective length of 280 m, a net width of 34
289 m, and a length of 280 m. At the Three Gorges Dam, south lock and ship lift can be used for
290 downstream ships, and north lock and ship lift can be used for upstream ships. At the Gezhouba
291 Dam, all three locks can be used by both upstream and downstream ships (**Fig. 4**).

¹ http://www.gov.cn/xinwen/2021-12/31/content_5665919.htm

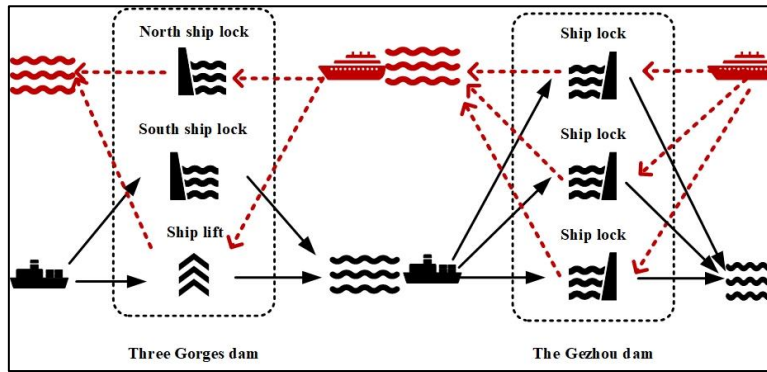


Fig. 4. Structure of the ship locks.

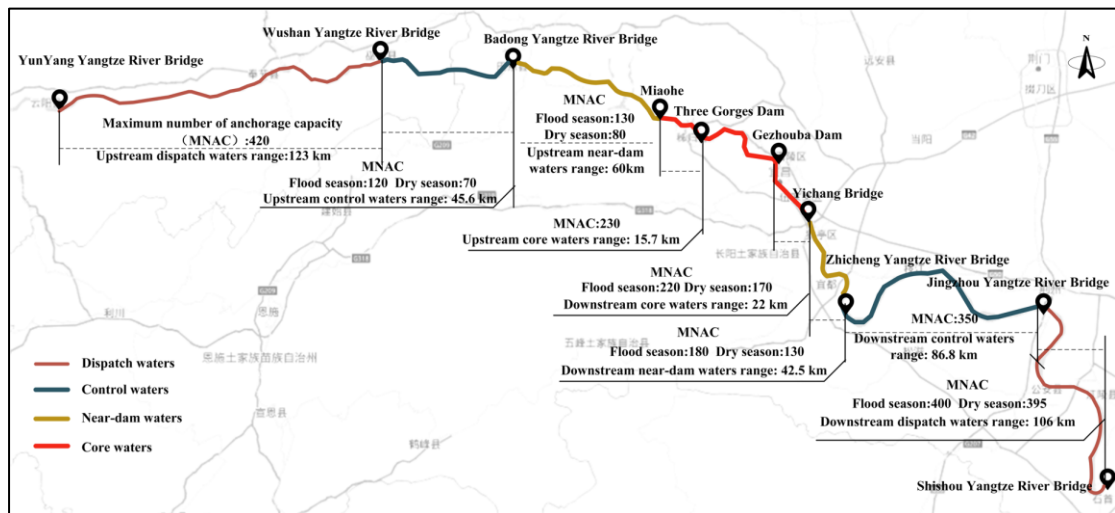


Fig. 5. Linkage control water area.

(1) Division of water areas

Linkage-controlled water area is divided into five areas based on its proximity to the Three Gorges dam: the core waters, near-dam waters, control waters, dispatch waters, and remote waters (Fig. 5).

1. Core waters: the waters in the middle reaches of the Yangtze River between the Yichang Yangtze River Highway Bridge (610.8 km in the middle reaches) and the Miaohe River (62.5 km in the upper reaches).

2. Near-dam waters: the waters between the Miaohe River and the Badong Yangtze River Bridge in the upper reaches of the Yangtze River (122.4 km in the upper reaches) and the waters between the Zhicheng Yangtze River Bridge and the Yichang Yangtze River Highway Bridge in the middle reaches of the Yangtze River (568.3 km in the middle reaches).

3. Control waters: the waters in the upper parts of the Yangtze River, between the Badong Yangtze River Bridge and the Wushan Yangtze River Bridge (168.0 km) and between the Jingzhou Yangtze River Bridge (481.5 km in the middle reaches) and the Zhicheng Yangtze River Bridge (481.5 km in the middle reaches).

4. Dispatch waters: the water area between the Wushan Yangtze River Bridge in the upper reaches and the Yunyang Yangtze River Bridge in the upper reaches and the water region between the Shishou Yangtze River Bridge in the middle reaches (375.5 km in the middle reaches) and the Jingzhou Yangtze River Bridge (291.3 km in the upper reaches).

5. Remote waters: the waters above the Yunyang Yangtze River Bridge and the waters below the Shishou Yangtze River Bridge on the Yangtze River's main trunk line.

3.4 Problem statement

318 (1) The TGGD water region is where ships often stop to wait for the lock according to the
 319 original traffic management plan. The capacity of the anchorage in the water region close to the dam
 320 cannot accommodate the demand for ship anchoring because of the steadily growing number of
 321 ships waiting for the lock, leading to a significant backlog of ships, channel congestion, scheduling
 322 issues, and other issues. Currently, it lacks a simulation model to test and verify the navigational
 323 effectiveness and traffic status of ships travelling through the dams under various traffic
 324 organisation schemes.

325 (2) The anchoring pressure in the water area close to the Three Gorges Dam has been
 326 significantly eased by traffic organisation, which has also significantly reduced congestion. A
 327 competent authority must dynamically adjust the number of anchorage and berthing areas along the
 328 route in the Linkage control water area because the anchorage and berthing areas along the
 329 Yunyang-Shishou water area are greatly affected by the change in water level in the wet and dry
 330 seasons. The width of the river surface in the wet season is greater than that in the dry season, and
 331 the depth of the anchorage and the area of the anchorage vary with the change in water level.

332 4. Efficiency quantification and modelling of ship traffic system

333 4.1 Configuration and definition

334 Under the new traffic organisation plan, ships must determine their next course of action based
 335 on the operational state of the navigation system. The functionality of the ship lock and the margin
 336 of anchoring along the way are the two key components of the system status. The ships sequentially
 337 berth at the anchorage along their routes because the system's continuous operation prevents the
 338 operational efficiency of the ship lock from meeting the needs of the ships going through the lock.
 339 Subsequent ships must dock at the anchorage further away from the ship lock when the anchorage
 340 closest to the ship lock is complete. We defined the parameters used to simplify modelling and
 341 computation, as shown in Table 1.

342 **Table1**
 343 **Parameter setting.**

<i>Classification</i>	<i>Variable</i>	<i>Definition</i>
<i>Three Gorges- Gezhouba navigation system</i>	A_d, A_c, A_{nd}	Anchorage in dispatch waters, control waters, near-dam waters
	$ A_n $	Anchorage capacity of anchorage n
	$A_{s,n}$	Moored ship quantity in anchorage n
<i>Ship dynamic system</i>	SL_{TG}	Ship lock in Three Gorges dam
	SL_G	Ship lock in Gezhouba dam
	S	Ship passing the ship lock
	$s_{t,l}$	State of ship s , include time t and location l
	$ S $	The number of ships passing the ship lock
	M	Optional action set provided to the ship
<i>Linkage control</i>	$m_{s,l}$	Action taken by ship s at location l
	P	Dispatch plan
	P_s	Dispatch plan of ship s
	U	Efficiency of navigation system
	T_a	Anchorage service level
	T_s	Saturation time of anchorage

344 4.2 Navigation efficiency quantification methods

345 In this study, we use s to represent ships, set the collection of ships as S , and use $|S|$ to

346 indicate the number of ships in lockage in accordance with the general method of ship lockage. In
 347 Eq. (1), P stands for the dispatching plan, which includes plan P carried out by ships when they
 348 are in motion, according to ship behaviour M . Location l and time t reflect the ship's state,
 349 whereas A stands for the anchorage, a_s stands for the capacity of A , \bar{a}_s represents the number of
 350 ships berthed in the anchorage.

$$\begin{aligned} m_{s,l} &= (t_{s,start}, l_s, t_{s,end}) \\ s_i &= (t, l), \quad i = 1, 2, 3, \dots, |S| \\ P_s &= \{m_{s,A_d}, m_{s,A_c}, m_{s,A_{nd}}\} \end{aligned} \quad (1)$$

351 The traffic efficiency of the TGGD U was altered as a result of the new traffic organisation
 352 scheme; however, new indicators and associated methodologies are required to assess the impact of
 353 the scheme's implementation. Consequently, in Eq. (2), we select the time T_a at which the
 354 anchorage reaches saturation, and the average waiting time T_s of the ship at each anchorage along
 355 the route. These two new indicators are used to assess the effectiveness of the navigation system
 356 and determine ways of improving the new traffic management plan based on changes in these two
 357 indicators.

$$U = (T_a, T_s) \quad (2)$$

358 In Eq. (3), T_a is a thorough indicator that can show the anchorage's service status along a route
 359 and the overall operating status of the navigation system, as seen from the anchorage. The longer
 360 the ship is waiting at the anchorage and the more serious the overall delay of the ship, the larger the
 361 value of T_a .

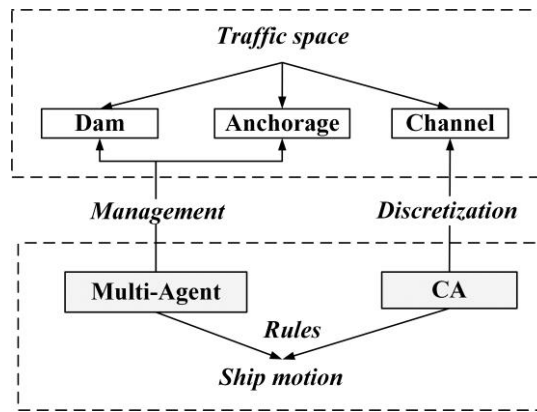
$$T_a = \frac{\sum_1^{|S|} t_{end,s}^a - t_{start,s}^a}{|S|} \quad (3)$$

362 In Eq. (4), T_s can be used to gauge the effectiveness of traffic-management strategies. The
 363 anchorage is likely to become saturated if the number of ships entering the anchorage increases
 364 faster than the rate at which they depart for the next anchorage. The anchoring approaches saturation
 365 later, and the system as a whole does so as T_s increases in value.

$$T_s = t_{end,s}^a, \quad \bar{a}_s = a_s \quad (4)$$

366 4.3 Modelling based on CA and multi-agent

367 T_a and T_s are indicators of how effectively ships navigate; it is, therefore, important to mimic
 368 the actual ship traffic flow during simulation. The entire complicated system can be reflected in and
 369 described using CA and multi-agent systems. For a multi-agent system, communication and
 370 coordination among agents are completed through a higher-level coordinator. By receiving
 371 instructions from the coordinator, agents make judgments according to their own knowledge base
 372 and characteristics and decide their own motion state. Although CA can greatly increase the
 373 simulation speed through the calculation mode of spatial-temporal discretisation and the running
 374 logic of synchronous calculation, it is challenging to simulate the interaction between traffic
 375 individuals and traffic facilities. Communication consumes a significant amount of system time and
 376 resources during the system operation. Given that the ship's motion state is updated through changes
 377 in cell state, and considering the advantages of the NaSch CA model - simplicity, ease of
 378 implementation, and effectiveness in describing traffic flow processes - we adopt the classical
 379 NaSch CA model as the foundation for this study. The cells representing the anchorage in the traffic
 380 system are expanded and improved, giving them the characteristics of agents that allow them to
 381 calculate their own service and despatch states. The operating logic of the synchronous computation
 382 of the CA is still used for the entire system, which means that every traffic entity's motion state is
 383 updated in the subsequent cycle to satisfy the simulation criteria for both speed and accuracy.



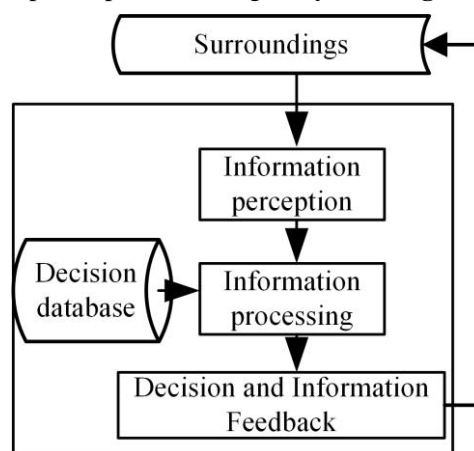
384
385
386 **Fig. 6. Structure of the model.**

387 Inspired by the linkage control scheme, a simulation model based on CA and multi-agents is
388 developed to simulate a large-scale navigation system composed of the TGGD and its upstream and
389 downstream navigable waters, as shown in Fig. 6. Studying the effectiveness of navigation and ship
390 delays under various traffic organisation schemes can help create groundwork for improving traffic
391 organisation.

392 An interactive particle system can be considered the behavioural logic of a multi-agent system.
393 The calculation amount of the agent model is greater than that of CA because it is important to
394 establish which agents an agent must interact with in the ongoing process. The simulation system is
395 expanded by leveraging agent thinking, and the anchorage and mooring areas are considered
396 essential nodes. The computation method for the anchorage agent is as follows:

- 397 a. Local environment sensing/neighbourhood sensing: collecting the state of the adjacent space
398 ships (cells) with the scheduling process of the control centre.
- 399 b. Make decisions and make the next scheduling plan for the anchorage.
- 400 c. Execute the scheduling plan and pass the information to the next node.

401 The agent needs to perceive the ship state and its own capacity in the surrounding cell space at
402 each moment and make scheduling decisions according to the overall scheduling rules of the
403 coordinating controller. As a result, the computational resources required for steps a and b are large.
404 One of the effective ways to improve the efficiency of local neighbourhood perception in a general
405 agent system is to arrange the agent positions in space in a certain way to achieve a 'regular'/
406 'ordered' state. The continuous spatial organisation of the CA model can structurally improve the
neighbourhood search and perception speed of the agent system. Fig. 7 shows the agent structure.

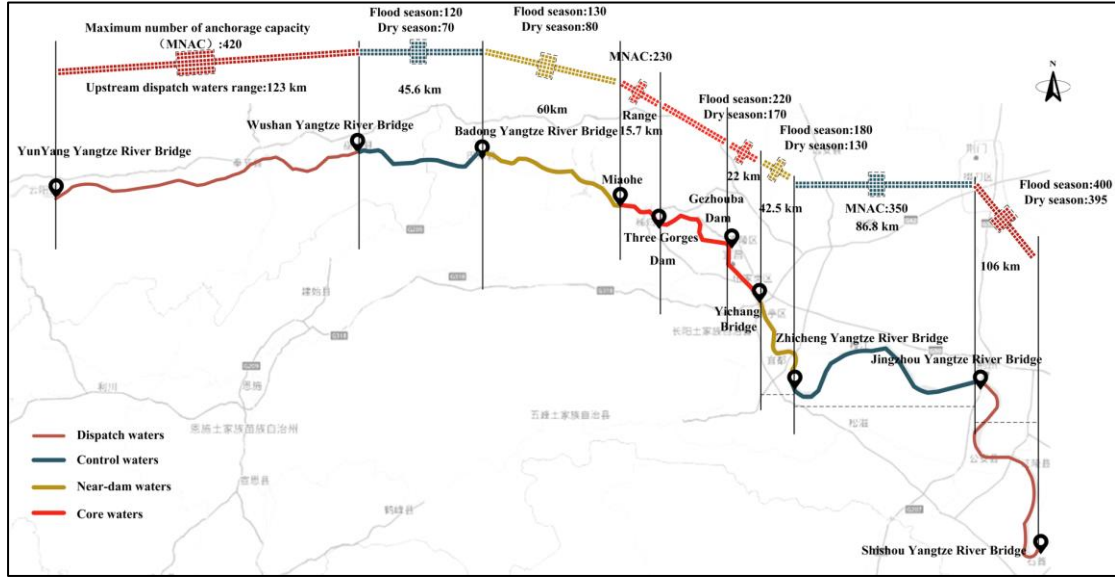


407
408 **Fig. 7. Structure of an agent.**

409 **5. Ship traffic simulation approach**

410 **5.1 Spatial-temporal discretisation**

411 In terms of time discretisation, scholars generally set the simulation time step in minutes in
 412 water traffic simulations because ships have larger scales and slower sailing speeds compared to
 413 vehicles. In the traffic model based on CA, the traffic space needs to be discretised, and it is
 414 generally believed that the way a ship occupies a cell is the most efficient one. In the ship traffic
 415 model, the safe distance between the same two ships d_{safe} ($d_{safe} = x_{n+1}(t) - x_n(t)$) must be
 416 considered. In two-dimensional cell space, the position of the ship is represented by $x(i, j)$, where
 417 i represents the lateral position, and j represents the position of the cell located in the channel.
 418 As the ship speed is in knots and the time step is in minutes, the cell size is set to $100\text{ m} \times 100\text{ m}$ in this
 419 model to reduce the computational intensity of the calculation, as shown in **Fig. 8**.



420
 421 **Fig. 8. Schematic representation of the structure of the model discretization.**

422

423 **5.2 Update rules**

424 In this model, the ship movement rules are designed based on the NaSch rules and the
 425 characteristics of ship traffic flow.

426 (1) Acceleration rules:

427 During normal navigation, if the distance between the front and rear ships is greater than the
 428 preset safe distance, $x_{n+1}(t) - x_n(t) > d_{safe}$, the rear ship will not be affected by the front ship.
 429 If the ship does not reach the maximum speed $v_n < v_{max}$, the ship will accelerate (Eq. (5)).

$$v_n \rightarrow \min\{v_n(t) + 1, v_{max}\} \quad (5)$$

430 (2) Deceleration rules

431 When the distance between $ship_n$ and $ship_{n+1}$ is less than the preset safe distance, $x_{n+1} -$
 432 $x_n < d_{safe}$, the rear ship needs to slow down (Eq. (6)).

$$v_n \rightarrow \min\{v_n(t) - 1, v_{min}\} \quad (6)$$

433 (3) Random slow

434 When a ship is sailing, it will inevitably be affected by wind, water currents, and visibility,
 435 which will reduce its speed. Therefore, it is necessary to add a random slowing variable a_{Δ} to the
 436 ship motion rules, and the value is determined according to the natural conditions in the channel
 437 (Eq. (7)).

$$v_n(t) = v_n(t - 1) - a_{\Delta} \quad (7)$$

438 (4) Location update rules

439 The ship's location update follows the rules shown in Eq. (8).

$$x_n(t+1) = x_n(t) + v_n(t) \quad (8)$$

440 (5) Changing lanes and overtaking rules

441 First, the motivation for lane change is judged according to the sorting of the scheme of the
442 front and rear ships and the sailing status of the front and rear ships. Generally, a normal sailing rear
443 ship will not overtake the front ship, but when the crossing plan of the rear ship precedes that of the
444 front ship i , $P_n < P_{n+1}$, the rear ship needs to change lanes, accelerate, and then overtake the front
445 ship.

446 Second, we determine the lane-changing conditions. If the speed of the front ship is lower than
447 that of the rear ship, $V_n(t) < V_{n+1}(t)$, and there is sufficient space in the adjacent channel, the lanes
448 are changed. After changing lanes, the rear ship needs to speed up to overtake the front ship. When
449 the distance between the front and rear ships reaches a safe distance that needs to be maintained,
450 $ship_{n+1}$ needs to turn into the original channel. The following rules should be followed during
451 overtaking:

452 Changing lanes rules are as shown in Eq. (9).

$$\begin{aligned} x_{n+1}(t) &= (t, 1) \\ x_{n+1}(t+1) &= (t, 2) \end{aligned} \quad (9)$$

453 Acceleration rules are as shown in Eq. (10).

$$v_{n+1}(t+\Delta t) = v_{n+1}(t) - a \Delta t \quad (10)$$

454 Return to the original channel rules are as shown in Eq. (11).

$$\begin{aligned} x_{n+1}(t+\Delta t) - x_n(t+\Delta t) &> d_{safe} \\ x_{n+1}(t+\Delta t+1) &= (t+\Delta t+1, 1) \end{aligned} \quad (11)$$

455 (6) Anchorage status change rules

456 The status of the anchorage can be represented by a binary variable. If there is at least one free
457 anchor, the variable is 1; if there is no free anchor, the variable is 0, as shown in Eq. (12).

$$S_{A_x,t} = \begin{cases} 1 & \text{if } \sum A_{x,t} < C_x \\ 0 & \text{if } \sum A_{x,t} = C_x \end{cases} \quad (12)$$

458 $S_{A_x,t}$ represents the status of anchorage A_x at time t ($x = d, c$ or nd), $A_{x,t}$ represents the
459 occupancy status vector of anchorage A_x at time t , and C_x is the total capacity of anchorage A_x .

460 When a ship enters the anchorage A_x , it can be expressed as Eq. (13)

$$F_{x,t+1} = \begin{cases} F_{x,t} - 1 & \text{if } F_{x,t} > 0 \\ F_{x,t} & \text{if } F_{x,t} = 0 \end{cases} \quad (13)$$

461 $A_{x,t}[i] = 1$ represents that the anchor i is occupied, $A_{x,t}[i] = 0$ represents that the anchor
462 i is free, and $F_{x,t}$ is the anchor idle counter.

463 The update of anchorage status $S_{A_x,t}$ can be expressed as Eq. (14)

$$S_{A_x,t+1} = \begin{cases} 1 & \text{if } F_{x,t+1} > 0 \\ 0 & \text{if } F_{x,t+1} = 0 \end{cases} \quad (14)$$

464 When a ship leaves the anchorage A_x , it can be expressed as Eq. (15)

$$F_{x,t+1} = F_{x,t} + 1 \quad (15)$$

465 The update of anchorage status $S_{A_x,t}$ can be expressed as Eq. (16)

$$S_{A_x,t+1} = 1 \quad (16)$$

466 5.3 Anchorage model based on multi-agents

467 To meet the requirement of anchorage simulation in the model, the homogeneity of the CA at
468 key nodes is improved, and the cells and their states are expanded. The cells in the same cell space
469 are classified, and the channel cells are still updated according to the basic rules, whereas the
470 anchorage cells have their own unique cell states, neighbours, and rules. To ensure that these
471 different states, neighbours, and rules still coordinate the same function as the whole system, we
472 can regard the cells representing the anchorage as separate individuals, package these cells and states

473 separately, and expand them into autonomous agents, with cell states as their attributes, so that
 474 different types of cells can act on the same cell space harmoniously.

475 In the actual process of a ship passing the lock, the Three Gorges Navigation Administration
 476 is responsible for the entire ship scheduling plan, and the Maritime Safety Administration along the
 477 ship's route is responsible for ship scheduling according to the site, as shown in **Fig. 9**.

478 (1) Remote declaration

479 After a ship is generated according to the ship generation rules, it is necessary to report the
 480 ship's passing plan to the Three Gorges Navigation Administration. The upstream and downstream
 481 ship reporting lines are the Shishou Yangtze River Bridge and the Yunyang Yangtze River Bridge,
 482 respectively. The time when ships go up through the Shishou Yangtze River Bridge or down through
 483 the Yunyang Yangtze River Bridge is the sequencing basis for making crossing plans. Ships are
 484 classified and sorted as dangerous goods, container, and commercial automobile transport ships,
 485 and a database of ship positions and statuses is established (Eq. (12)).

$$S = \begin{bmatrix} s_1 = (l, t) \\ s_2 \\ \vdots \\ s_i \\ s_{i+1} \\ \vdots \\ s_{|S|} \end{bmatrix} \quad (12)$$

486 The scheduling plan of all ships can be expressed as P_S shown in Eq. (13).

$$P_S = \begin{bmatrix} P_1 = \{m_{1,A_d}, m_{1,A_c}, m_{1,A_{nd}}\} \\ P_2 \\ \vdots \\ P_s \\ P_{s+1} \\ \vdots \\ P_{|S|} \end{bmatrix} \quad (13)$$

487

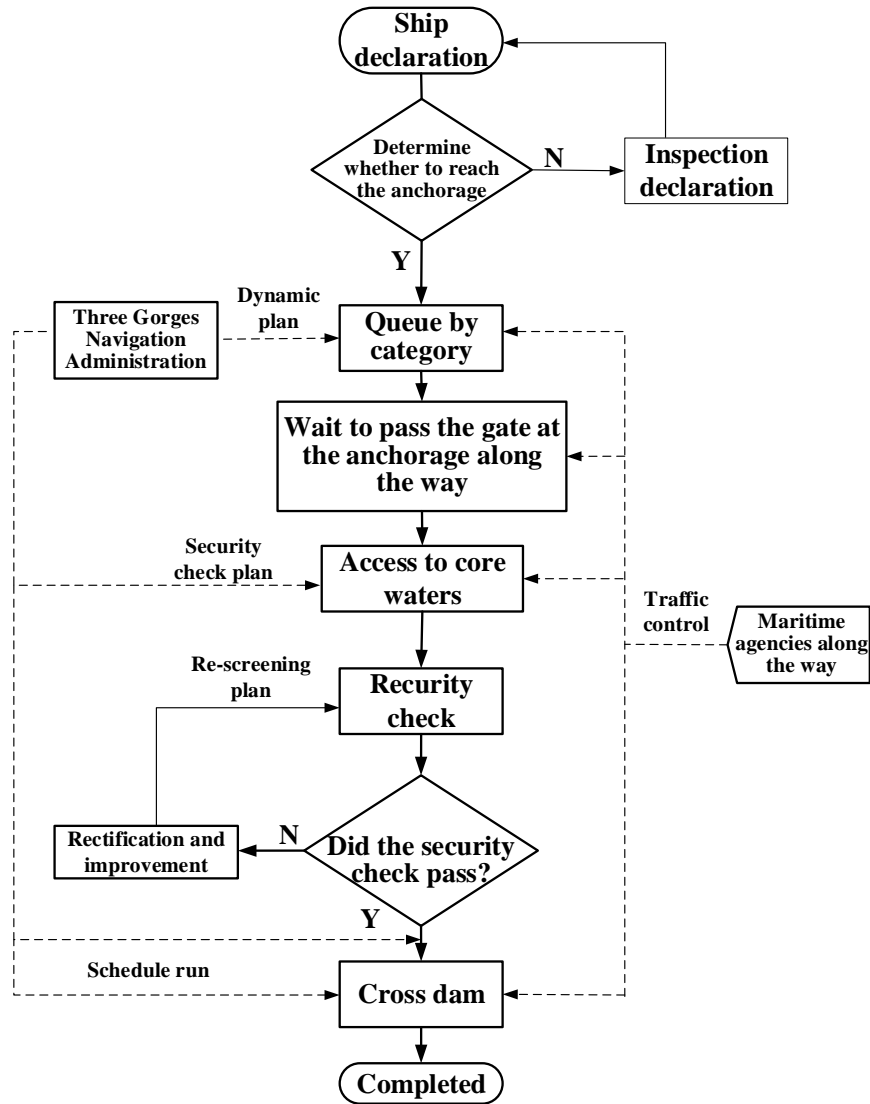


Fig. 9. Traffic organisation flowchart of a ship passing a ship lock.

(2) Scheduling along line

After a ship arrives at the anchorage along its route, it is necessary to update the ship status database based on its position and status (Eq. (14)). The Maritime Safety Administration along its route will reorder and release the anchored ships on the spot according to the ship sequencing plan issued by the Three Gorges Navigation Administration. To achieve this goal, it is necessary to compare the state database with the sequencing plan and establish a new scheduling plan.

$$A_{s,n} = \begin{bmatrix} s_i(l_{A_n}, t) \\ \vdots \\ s_{i+x}(l_{A_n}, t) \\ \vdots \end{bmatrix} \quad (14)$$

(3) Security inspection of the water near the dam

A safety inspection is required when ships reach the water near the dam. Qualified ships will continue to wait in line, and unqualified ships will need to return to nearby anchorages for rectification (Eq. (15)). Only after passing the inspection can they continue to queue to pass the ship lock. Decision-making and perception libraries are established in the agent model to realise this process.

$$\begin{aligned}
A_{s,c} &= \begin{bmatrix} s_i(l_{A_c}, t) \\ \vdots \\ s_{i+x}(l_{A_c}, t) \\ \vdots \end{bmatrix} + \begin{bmatrix} s_{d,1}(l_L, t) \\ \vdots \\ s_{d,|D|}(l_L, t) \\ \vdots \end{bmatrix} \\
P_S &= \begin{bmatrix} P_1 = \{m_{1,A_d}, m_{1,A_c}, m_{1,A_{nd}}\} \\ P_2 \\ \vdots \\ P_i \\ P_{i+1} \\ \vdots \\ P_{s_{d,1}} \\ P_{s_{d,|D|}} \\ \vdots \\ P_{|S|} \end{bmatrix}
\end{aligned} \tag{15}$$

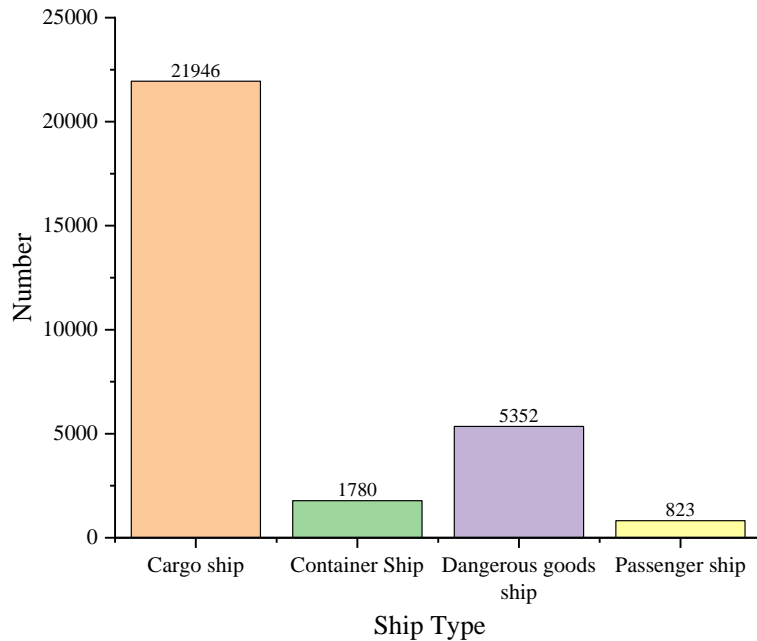
502 **6. Experiment and results**

503 **6.1 Traffic flow characteristic analysis**

504 In this study, the data of ships that passed through the TGGD in 2018 are analysed, and the
505 characteristics of ship traffic flow required for simulation are obtained from the data, including ship
506 type distribution, ship length distribution, and ship speed distribution.

507 (1) Distribution of ship types

508 From the statistical data of ship traffic flow, it is found that the ships that passing through the
509 linkage-controlled water mainly include bulk carriers, general cargo ships, general dry cargo ships,
510 multipurpose ships, oil tankers, and chemical tankers. From the perspective of ship characteristics,
511 bulk carriers, general cargo ships, and general dry cargo ships can be regarded as cargo ships.
512 Therefore, four main ship types were selected in this study: container ships, dangerous goods ships,
513 passenger ships, and cargo ships, as shown in **Fig. 10**. Their specific generation rules refer to the
514 actual statistical distribution of ship types in 2018.



515

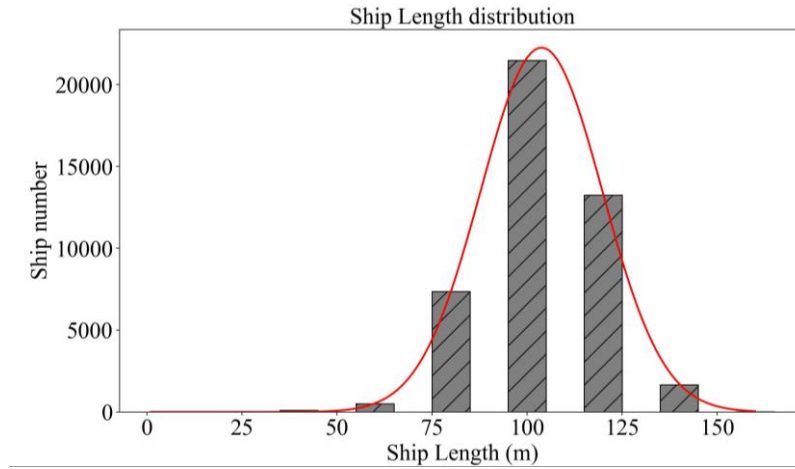
516

Fig. 10. Distribution of ship types.

517 (2) Distribution of ship length

518 By analysing the ship scale, it can be found that the length of ships in the waters controlled by

519 linkage is mostly between 60 and 140 metres, of which 80–100 m ships account for 48.4%, as shown
 520 in **Fig. 11**. Therefore, when ships are generated in the simulation system, the ship length distribution
 521 obeys a normal distribution, with an R-square of 0.98 and a standard deviation of 22.6.



522
 523 **Fig. 11. Distribution of ship length.**

524 (3) Distribution of ship speed

525 Ship speed distribution refers to the speed distribution range and patterns of all ships sailing in
 526 a certain water area. The ship's speed distribution is affected by the navigation environment and the
 527 ship's own attributes, but the ship speed mostly obeys a normal distribution.

$$f(v) = \frac{1}{\sqrt{2\pi}\sigma} e^{-\frac{(v-\mu)^2}{2\sigma^2}} \quad (16)$$

528 where $f(v)$ represents the probability that the ship speed is v , σ represents the standard deviation
 529 of the ship speed in the water, and μ represents the average speed of the ship in the water.

530 The speed of the ship is different under different traffic flows. Through an analysis of the traffic
 531 flow data of ships in the linked control waters from September to October 2018, the downstream
 532 ship speed is mostly between 10–20 km/h and the upstream ship speed is mostly between 4-10 km/h.
 533 By fitting the speed data of ships in the linked control waters, the speed distribution of inland river
 534 ships conforms to a normal distribution, and thus the ship speed generated in the simulation model
 535 obeys the normal distribution. The ship speed data of Yunyang and Shishou are selected as examples,
 536 and Eq. (16) is used to fit the ship speed. The results are shown in **Fig. 12** and the specific parameters
 537 are listed in Table 2.

538 **Table 2**

539 **Parameters generated during fitting of the ship speed.**

	Downstream	Upstream
R-square	0.9873	0.9395
Standard deviation	1.904	1.051

540

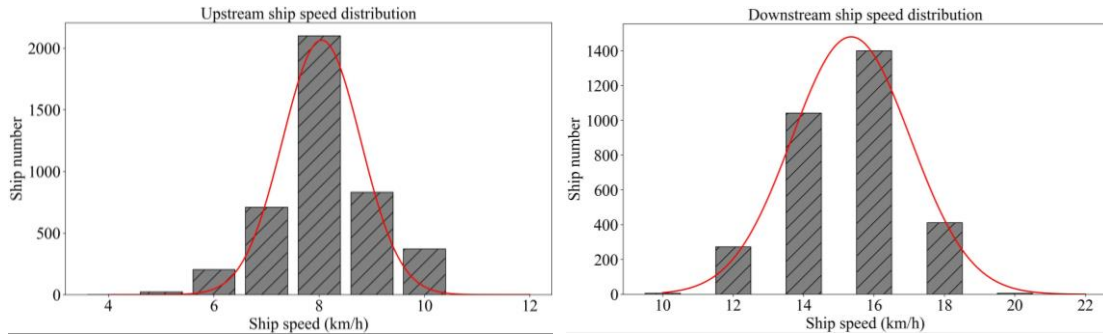


Fig. 12. Fitting of the ship distribution.

6.2 Parameter setting

According to the traffic flow characteristics of ships passing the lock in 2018, the ship generation rules in the simulation model are set, including ship type distribution, ship size distribution, speed change range, and other related parameters. The bearing capacity of the key nodes in the simulation model is set according to the distribution of anchorages and berthing areas along the water area under linkage control.

The channel is discretised according to specific information, such as the overall length and width of the linkage control segment and the rules of the CA. The total length of the channel is approximately 541 km, the average channel width is approximately 75 m, and the length of the ship is approximately 100 m. If the size of one cell in the cell space is determined to be 100 m × 100 m, the entire channel is divided into 5,410 cells. According to the specific situation of the Yangtze River waterway and the setting of ship berthing areas, the entire cellular space is divided into three parts: the regions above the Three Gorges Dam, between the Three Gorges Dam and the Gezhouba Dam, and below the Gezhouba Dam. The cellular space above the Three Gorges Dam is subdivided into four areas according to the location of each anchorage. The cellular space below the Gezhouba Dam is subdivided into four areas according to the location of each anchorage, as listed in Tables 3 and 4.

Table 3

Upstream Channel Discretisation.

Segment	Remote waters	Dispatch waters	Control waters	Near-dam waters	Core waters
Cell number	1230	460	600	170	380

Table 4

Downstream Channel Discretisation.

Segment	Near-dam waters	Control waters	Dispatch waters	Remote waters
Cell number	220	420	870	1060

In the anchorage setting, the simulation of the entire channel will encapsulate the anchorage cell of the same segment, and the reference to the capacity of anchorage everywhere will represent the location of the cell setting of the anchorage multi-agent as well as the capacity, as listed in Tables 5 and 6.

Table 5

Upstream Anchorage capacity.

Location	Dispatch waters	Control waters	Near-dam waters	Core waters
----------	-----------------	----------------	-----------------	-------------

Dry season	420	70	80	220
Flood season	420	120	130	220

570 **Table 6**
571 **Downstream Anchorage capacity.**

Location	Core waters	Near-dam waters	Control waters	Dispatch waters
Dry season	170	130	350	395
Flood season	220	180	350	400

572 The simulation adopts a finite boundary, the simulation range of downstream ships is set from
573 Yunyang to Three Gorges Dam, and the simulation range of upstream ships is set from Jingzhou to
574 Gezhouba.

575 **6.3 Model validation**

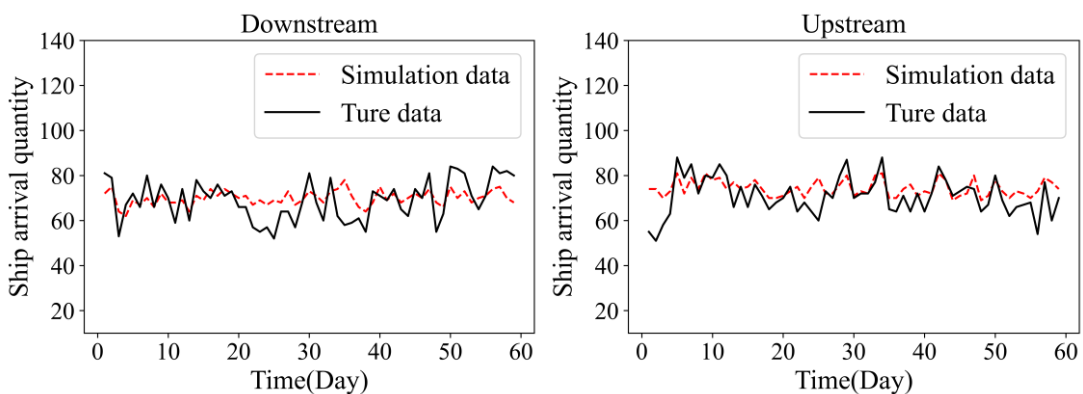
576 To verify that the simulation model can truly reflect the actual navigation status of ships in
577 linkage control waters, the actual traffic flow data were compared with the data derived from the
578 simulation run. After the model ran steadily, the reliability of the model was verified in terms of the
579 number of upstream and downstream ships arriving at the Yunyang Yangtze River Bridge and the
580 Shishou Bridge and the number of ships passing through the Three Gorges Locks; the results are
581 presented in Table 7 and **Fig. 13**.

582
583

584 **Table 7**
585 **Verification of the number of arriving ships.**

Type	Upstream	Downstream
Actual number of ship arrivals	4243	4145
Number of simulated ship arrivals	4348	4204
Error	105 (2.5%)	59(1.4%)

586



587

588 **Fig. 13. Verification of the number of arriving ships.**

589 Comparing the simulation results with the actual traffic flow data, it can be seen that the
590 number of ships generated by the simulation is relatively stable, the actual number of ships is more
591 random in the course of sailing, and some ships have some illegal behaviours such as non-
592 compliance with navigation regulations, which changes the actual number of arriving ships
593 significantly. From Table 7, the errors of the upstream and downstream ships are 2.5% and 1.4%,

594 respectively. Because inaccuracy is minimal, ship generation can be considered plausible.

595 **Table 8**

596 **Verification of the number of ships passing through gates.**

Type	Upstream	Downstream
Actual number of ships passing through ship lock	4172	4082
Simulation of the number of ships passing through the ship lock	3906	3793
Error	266 (6.4%)	289 (7.1%)

597 As can be seen from Table 8, during the 30-day simulation, the actual number of upstream
 598 ships passing through the ship lock was 4,172, the simulated number of ships passing through the
 599 ship lock was 3,906, with a relative error of 6.4%, the actual number of upstream ships passing
 600 through the ship lock was 4,082, and the simulated number of ships passing through the ship lock
 601 was 3,793, with a relative error of 7.1%. As there is a difference between the actual ship crossing
 602 behaviour and the abstract ship crossing behaviour in the simulation, the acceptable error was within
 603 10%. Considering the environmental impact, driver behaviour and psychology, special
 604 circumstances, and other influencing factors in the actual sailing process, this model was considered
 605 to have high reliability and can accurately and truly reflect the navigation state of ships in the linked
 606 control waters.

607 **6.4 Results and analysis**

608 Based on the historical operation of the TGGD navigation system, we set up four scenarios in
 609 the simulation.

610 In Scenario 0, the linkage control scheme has not been implemented for the navigation system
 611 of the TGGD before 2017.

612 In Scenario 1, the linkage control scheme for the navigation system of the TGGD has been
 613 implemented. The period that is simulated is that after 2017.

614 In Scenario 2, the linkage control scheme of the TGGD navigation system has been
 615 implemented, and the ship traffic flow density further increases.

616 In Scenario 3, there is a change in anchorage capacity with the water level in the flood and dry
 617 seasons in the linkage control scheme area when the ship traffic flow density is further increased.

618 **Table 9**

619 **Simulation Scenarios.**

Scenario	Linkage control scheme	Change of traffic flow	Change of anchorage
Scenario 0:	-	-	-
Scenario 1:	√	-	-
Scenario 2:	√	√	-
Scenario 3:	√	√	√

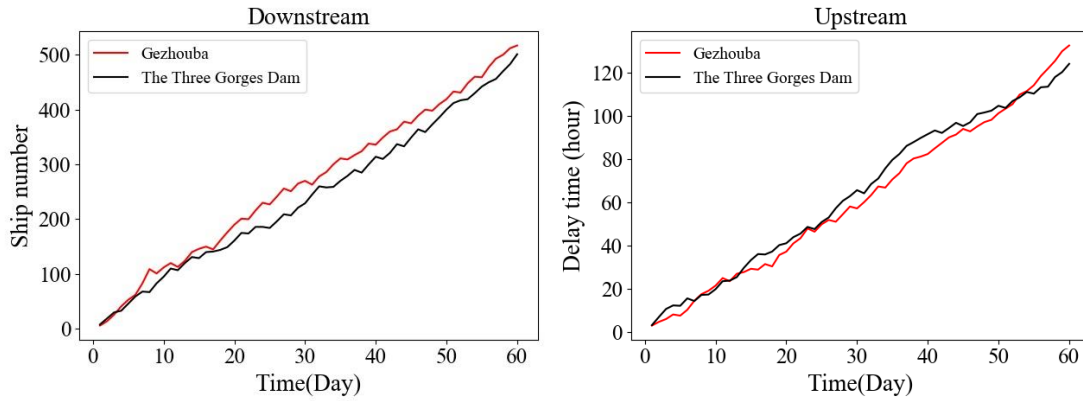


Fig. 14. States of a ship waiting to pass the lock.

According to the experimental results shown in Fig. 14, the situation of ship delay before the implementation of the linkage control scheme presents the following characteristics:

a. Ships crossing the lock sail directly to the core waters to wait for the lock. Over a period, too many ships arrive at the lock, causing channel blockage, and the ship-carrying capacity of the lock exceeds the navigation capacity of the hub.

b. The number of ships waiting to lock in the core waters fluctuates within a small range owing to the number of ships generated; however, owing to the traffic flow capacity and lock restrictions, the time and number of ships waiting to lock in front of the dam will continue to increase with time. After 60 days of simulation, the number of ships berthing and waiting for the gate reaches approximately 510, and the average waiting time reaches approximately 130 h.

c. All ships are overstocked in the waters in front of the dam prior to the implementation of the linkage control scheme, especially when the carrying capacity of the lock is reduced during the overhaul period and the carrying capacity of the waterway in the dry season. The problem of insufficient carrying capacity of the TGGD will be further highlighted.

As shown in Fig. 15, the ships arriving at dispatch water apply the linkage control scheme, obtain the relevant dispatching orders, and then wait in a timely manner in the anchorage and berthing areas. The ships waiting to pass through the gate typically exhibit the following characteristics:

1) The rate of saturation of the anchorage and mooring area along the route is inversely related to the distance from the core water region. The descending ships progressively stop at all berthing places along the way as the number of ships travelling through the lock continues to rise. The core water area is the first to reach saturation, and the farther away a water area from the core water area, the slower is its rate of saturation.

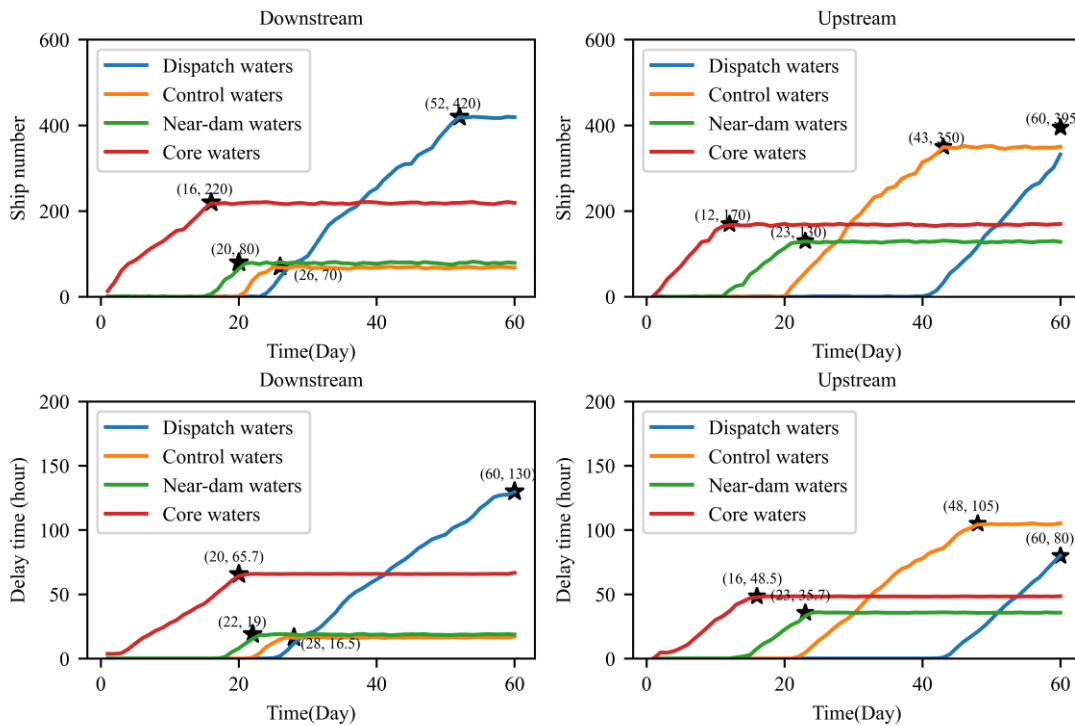
2) The capacity of each anchorage is positively related to the time that the downstream ships wait. The average wait time for ships leaving an anchorage increases with capacity. The number of ships waiting to be locked in the core waters decreased from 510 to 220 because of the implementation of the linkage control plan, and the average waiting period decreased from 130 h to roughly 65 h. The strain on the core waters significantly decreased as a result of the linking control scheme implementation, and the descending ships are now more organised.

3) The trend of the upstream ship waiting to pass the lock is the same as that of the downstream ship. The capacity of the berthing area causes each anchorage along the route to become saturated, and the average waiting time of ships at each anchorage is tied to that capacity. In particular, the downstream dispatch water anchorage is not saturated after 60 days of simulation running, and the average waiting time for ships in the anchorage did not reach the maximum value. In general, after the implementation of the linkage control plan, the berthing situation in the Gezhouba dam waters region has also been greatly eased, the number of waiting ships is greatly reduced, and the pressure

658 on on-site supervision and ship safety risks is reduced.

659 **6.4.1 Scenario 1**

660



661

662

Fig. 15. Experimental result of Scenario 1.

663 **6.4.2 Scenario 2**

664 Increasing the demand for ships passing through locks increases the density of ships.
665 According to the on-the-spot investigation and analysis of the traffic flow data of ships in the TGGD
666 navigation system in recent years, the number of ships passing through the joint control waters is
667 increasing annually, and the number of ships that passed through the lock in 2021 was increased by
668 9.29% year-on-year. It is predicted that the number of ships passing through the TGGD will increase
669 steadily in the future. To study the situation of ships waiting for lockage in the berthing areas of
670 each water area of the linkage control segment under the heavy lockage demand, we can convert
671 the lockage demand of ships into the traffic flow of ships and adjust the ship generation parameters
672 to increase the number of ships generated every day by 20% for the simulation.

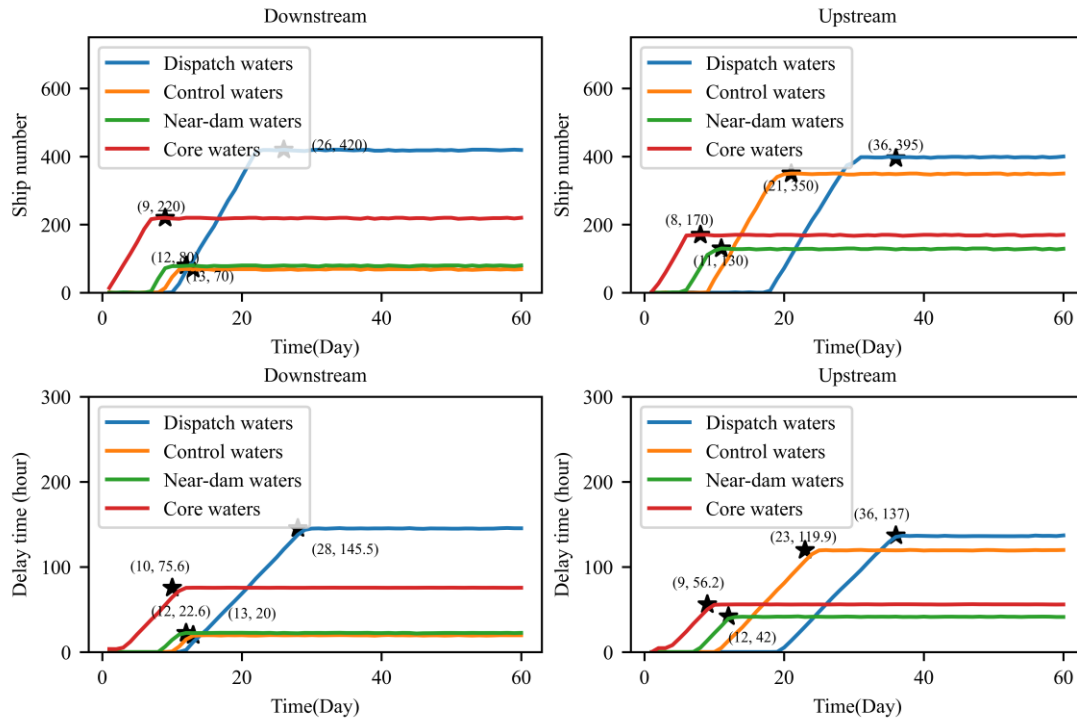
673 When comparing the experimental results shown in **Fig. 16** with the initial results following
674 the increased demand for ships transiting the locks, it was discovered that:

675 1) Because the capacity of the anchorage and berthing areas has not changed, increasing the
676 demand for ships to pass the lock has little effect on the number of ships waiting to pass the lock
677 when the berthing area of each voyage is saturated.

678 2) The start time of the ship backlog is affected by the distance between the anchorage and
679 lock. The greater the distance, the greater is the impact on the backlog start time. The start time of
680 the backlog of ships in the core waters was almost unchanged, and the start time of the backlog of
681 ships in the waters near the dam was approximately eight days earlier. The mooring area in the
682 dispatch waters is most affected by the change in the demand for ships to pass the gate, and the
683 backlog of ships starts approximately 23 days earlier.

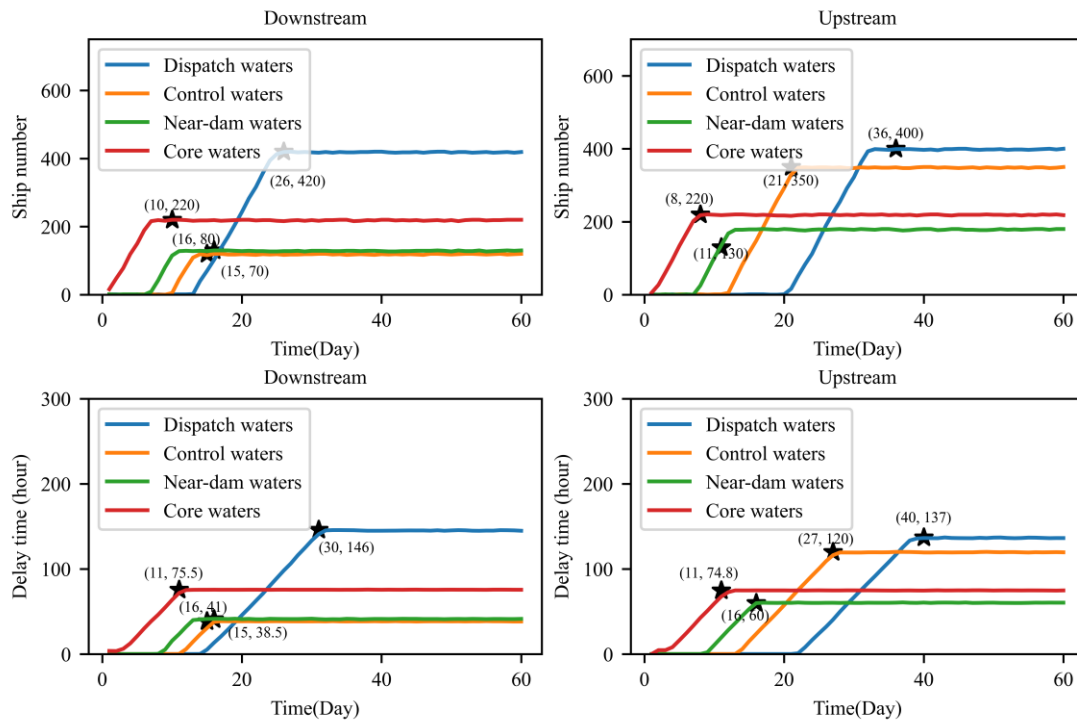
684 3) The anchorage in the originally unsaturated downstream dispatch water begins to operate at
685 full capacity. The average layoff delay of ships waiting at anchorages is approximately 135 h.

686 Overall, the average waiting time of the ships in each berthing area increased to various degrees. It
 687 can be seen that the average waiting time of ships in the anchorage is affected by both the capacity
 688 of the anchorage and the demand for ships to pass through the lock.



689
690 **Fig. 16. Experimental results for Scenario 2.**

691 **6.4.3 Scenario 3**



692
693 **Fig. 17. Experimental results for Scenario 3.**

694 From the simulation results shown in Fig. 17, it can be found that:

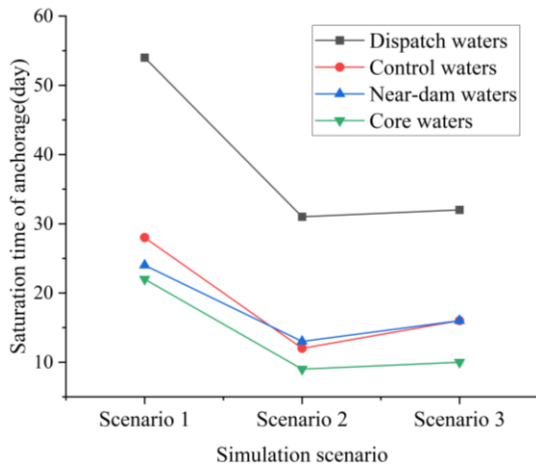
- 695 1) The start time of the backlog of ships will be slightly delayed, with an average delay of

696 approximately five days, in the upstream dispatch waters, downstream control waters, and dispatch
 697 waters. Therefore, the demand for anchorages along the routes that are operating at full capacity
 698 will be reduced by expanding the capacity of the selected anchorages.

699 2) The average waiting time of ships in the upstream Control waters increased from 20 h to
 700 approximately 39 h, the average waiting time of ships in the upstream Near-dam waters increased
 701 from approximately 23 h to 43 h, the average waiting time of ships in the downstream Near-dam
 702 waters anchorage increased from 42 h to 60 h, and the average waiting time of ships in the
 703 downstream Core waters increased from 56 h to 75 h, further verifying that the average waiting
 704 time of ships at each anchorage is positively correlated with the anchorage capacity.

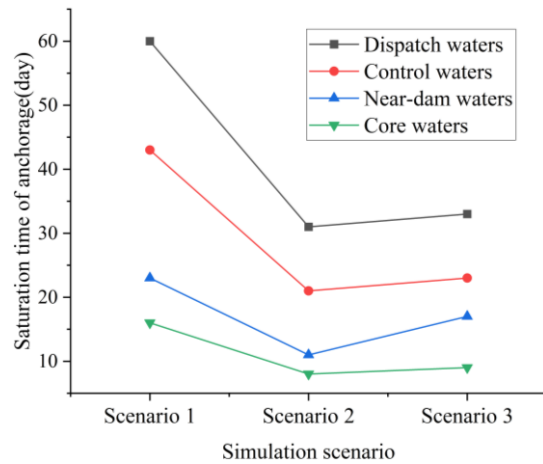
705 **7. Discussion and conclusion**

706 **7.1 Discussion**



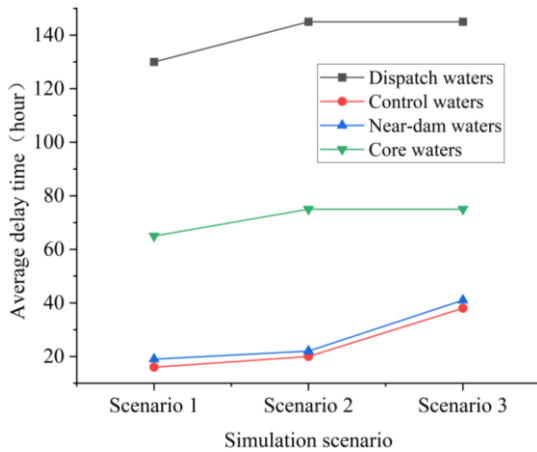
707

a. Saturation time at anchorages above the Three Gorges



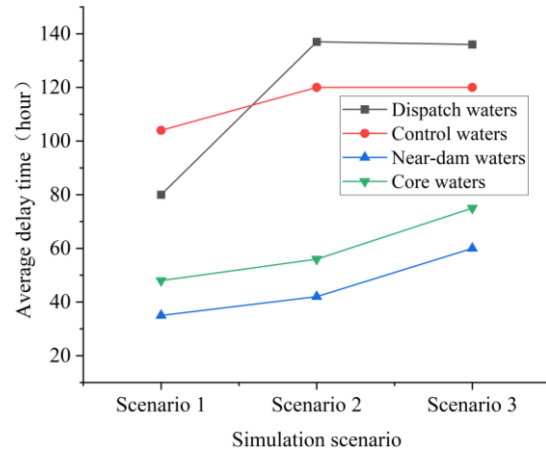
b. Saturation time of anchorage below Gezhouba Dam

708



709

c. Maximum delay time for downward ships



d. Maximum delay time for upward ships

710 **Fig 18. Saturation times at anchorages and the maximum delay times.**

711 The comparison and analysis of the outcomes before and after the adjustment reveal that while
 712 an increase in the number of ships and their delay times is a natural phenomenon (Fig. 18), it will
 713 lessen the backlog in the remote-controlled area. This is because of the increased anchorage in the
 714 waters near the dam and the dispatch waters. The specific performance is a delay at the beginning
 715 of the ship backlog and a reduction in the number of backlogged ships. Therefore, one of the steps

716 that can be implemented to reduce the backlog in remote waters is to increase the anchorage capacity
717 in dispatch and near-dam waters.

718 After reviewing the experimental findings, we identified several issues with the linkage control
719 strategy. Consequently, we provide a few optimisation ideas for the linkage control scheme for the
720 administrative organisation by combining the trial results with the actual operation scenario.

721 Firstly, we discovered that the ship lock pass plan and the present security check plan of the
722 TGGD are improvable. Currently, the Three Gorges Dam implements a 100% security check policy,
723 which requires ships that do not pass the inspection to return to the anchorage for rectification.
724 However, the vacant lock slots cannot be filled with new ships because the number of ships going
725 to the security inspection area each day is the same as the number of lock slots available. This leads
726 to a waste of lock resources. We believe there are some methods to alleviate this problem, such as
727 arranging 10%-20% more ships to go to the inspection area each day to avoid waste, and this ratio
728 can be dynamically adjusted based on the proportion of ships that did not pass the inspection the
729 previous day. Additionally, improving the efficiency of security checks by using information
730 technology can also help address this issue.

731 Secondly, our experiments revealed that under a certain ship traffic flow density, remote
732 anchorages from the dam do not reach saturation. Consequently, overextending the water area range
733 for linkage control is imprudent. However, water level changes affecting anchorage capacity
734 necessitate expanding the linkage control water area range to alleviate ship waiting times. Thus,
735 dynamic adjustment of water area ranges under linkage control is beneficial for managing varying
736 traffic conditions.

737 **7.2 Conclusion**

738 In this study, a hybrid simulation modelling approach combining Cellular Automaton (CA)
739 and Multi-Agent methods is proposed to analyse ship traffic through Waterway Transport Key
740 Nodes (WTKNs). This approach employs CA to accurately simulate dynamic traffic on various
741 waterways and utilizes multi-agent theory to manage anchorages effectively. The mathematical
742 model developed is particularly adept at representing the critical role that key nodes play within the
743 navigation system and their impact on navigation efficiency. By dynamically modelling the
744 operational state with ships navigating through locks under diverse traffic schemes, our model offers
745 insights into key operational conditions such as the maximum average waiting time at anchorages
746 and saturation periods. Simulation results affirm that our model's capability to adjust anchorage
747 capacities and water area ranges under linkage control effectively manages traffic conditions and
748 fluctuations. This highlights the model's robust utility in enhancing decision-making for optimising
749 traffic organisation at waterway transport key nodes.

750 This study presents a novel conceptual approach for analysing a large-scale, multi-key-node
751 traffic system by simulating the traffic of a navigation system of this type for the first time, with a
752 specific focus on ship traffic flow. Due to the modular structure of the proposed model, it can be
753 adapted to different requirements, thus enabling its application in studying the traffic efficiency of
754 other navigation systems with similar critical traffic nodes. Subsequent studies will further
755 investigate the impact of individual ship behaviour on traffic efficiency and aim to enhance the
756 accuracy of the model.

757 **Acknowledgement**

758 This study was supported by the National Natural Science Foundation of China (No.
759 51709219), Chinese Academy of Engineering and regional cooperation projects (No. HB2022B22),
760 and Qingdao Research Institute of Wuhan University of Technology (No.:2019A02).

761 **References**

762 Agussurja, L., Kumar, A., & Lau, H. C., 2018, April. Resource-constrained scheduling for maritime

763 traffic management. In Proceedings of the AAAI Conference on Artificial Intelligence (Vol.
764 32, No. 1), <https://doi.org/10.1609/aaai.v32i1.12086>.

765 Almaz, O. A., & Altiok, T., 2012. Simulation modeling of the vessel traffic in Delaware River:
766 Impact of deepening on port performance. *Simulation modelling practice and Theory*, 22, 146-
767 165, <https://doi.org/10.1016/j.simpat.2011.12.004>.

768 Aydogdu, Y. V., Yurtoren, C., Park, J. S., Park, Y. S., 2012. A study on local traffic management
769 to improve marine traffic safety in the Istanbul Strait. *The Journal of Navigation*, 65(1), 99-
770 112, <https://doi.org/10.1017/S0373463311000555>.

771 Biham, O., Middleton, A. A., Levine D., 1992. Self-organization and a dynamical transition in
772 traffic-flow models. *Physical Review A*, 46(10), R6124.

773 Bokus-Roszkowska, A., Smolarek, L., 2014. Maritime traffic flow simulation in the intelligent
774 transportation systems theme. In: *Safety and Reliability: Methodology and Applications-*
775 *Proceedings of the European Safety and Reliability Conference (ESREL 2014)*, Sep. 14-18,
776 2014, WROCLAW, POLAND.

777 Carse, A., 2012. Nature as infrastructure: Making and managing the Panama Canal watersh
778 ed. *Social Studies of Science*, 42(4), 539-563, <https://doi.org/10.1177/0306312712440166>.

779 Chen, Q., Yi, J., Wu, Y., 2019. Cellular automaton simulation of vehicles in the contraflow left-turn
780 lane at signalised intersections. *IET Intelligent Transport Systems*, 13(7), 1164-1172,
781 <https://doi.org/10.1049/iet-its.2018.5451>.

782 Deng, Y., Sheng, D., Liu, B., 2021. Managing ship lock congestion in an inland waterwa
783 y: A bottleneck model with a service time window. *Transport Policy*, 112, 142-161, h
784 <https://doi.org/10.1016/j.tranpol.2021.08.017>.

785 Deo, P., Ruskin, H., 2014. Urban Signalised Intersections: Impact of Vehicle Heterogeneity
786 and Driver Type on CrossTraffic Maneuver's. *Physical* 405(3), 140–150, <http://dx.doi.org/10.1016/j.physa.2014.02.078>.

788 Souza, F.d., Verbas, O., Auld, J., 2019. Mesoscopic traffic flow model for agent-based si
789 mulation. *Procedia Comput. Sci.* 151, 858–863, <https://doi.org/10.1016/j.procs.2019.04.1>
790 18.

791 Fan, S., Yang, Z., Wang, J., Marsland, J., 2022. Shipping accident analysis in restricted w
792 aters: Lesson from the Suez Canal blockage in 2021. *Ocean Engineering*, 266, 11311
793 9, <https://doi.org/10.1016/j.oceaneng.2022.113119>.

794 Feng, H., 2013. Cellular automata ship traffic flow model considering integrated bridge system. *Int.*
795 *J. u- e- Serv. Sci. Technol.* 6, 121–132. <https://doi.org/10.14257/ijunesst.2013.6.6.12>.

796 Fujii, H., Uchida, H., Yoshimura, S., 2017. Agent-based simulation framework for mixed traffic of
797 cars, pedestrians and trams. *Transportation research part C: emerging technologies*, 85, 234-
798 248, <https://doi.org/10.1016/j.trc.2017.09.018>.

799 Goerlandt, F., Kujala, P., 2011. Traffic simulation based ship collision probability modellin
800 g. *Reliability Engineering & System Safety*, 96(1), 91-107, <https://doi.org/10.1016/j.res.2010.09.003>.
801 2010.09.003.

802 Hu, H., Chen, X., Sun, Z., 2017. Effect of water flows on ship traffic in narrow water ch
803 annels based on cellular automata. *Polish Maritime Research*, 24(S3 (95)), 130-135, ht
804 [tps://doi.org/10.1515/pomr-2017-0115](https://doi.org/10.1515/pomr-2017-0115).

805 Jiang, L., Huang, G., Huang, C., Wang, W., 2019. Data mining and optimization of a port vessel
806 behaviour behavioural model under the Internet of Things. *IEEE Access* 7, 139970–139983,
807 10.1109/ACCESS.2019.2943654.

808 Karaaslan, E., Noori, M., Lee, J., Wang, L., Tatari, O., Abdel-Aty, M., 2018. Modeling th
809 e effect of electric vehicle adoption on pedestrian traffic safety: An agent-based appro
810 ach. *Transportation Research Part C: Emerging Technologies*, 293: 198-210, <https://doi.org/10.1016/j.trc.2018.09.003>.

811 [org/10.1016/j.trc.2018.05.026](https://doi.org/10.1016/j.trc.2018.05.026).

812 Ksciuk, J., Kuhlemann, S., Tierney, K., Koberstein, A., 2023. Uncertainty in maritime ship
813 routing and scheduling: A Literature review. *European Journal of Operational Research*,
814 308(2), 499-524, <https://doi.org/10.1016/j.ejor.2022.08.006>.

815 Köse, E., Başar, E., Demirci, E., Güneroğlu, A., Erkebay, Ş., 2003. Simulation of marine t
816 raffic in Istanbul Strait. *Simulation Modelling Practice and Theory*, 11(7-8), 597-608.
817 <https://doi.org/10.1016/j.simpat.2003.10.001>

818 Li, Z., Huang, H., Yang, H., 2020. Fifty years of the bottleneck model: A bibliometric re
819 view and future research directions. *Transportation research part B: methodological*, 13
820 9, 311-342, <https://doi.org/10.1016/j.trb.2020.06.009>.

821 Liu, B., Li, Z. C., Sheng, D., Wang, Y., 2021a. Integrated planning of berth allocation an
822 d vessel sequencing in a seaport with one-way navigation channel. *Transportation Res
823 earch Part B: Methodological*, 143, 23-47, <https://doi.org/10.1016/j.trb.2020.10.010>.

824 Liu, B., Li, Z. C., Wang, Y., Sheng, D., 2021b. Short-term berth planning and ship sched
825 uling for a busy seaport with channel restrictions. *Transportation Research Part E: Lo
826 gistics and Transportation Review*, 154, 102467, <https://doi.org/10.1016/j.tre.2021.102467>
827 7.

828 Liu, Y., Liu, J., Zhang, Q., Liu, Y., Wang, Y., 2024. Effect of dynamic safety distance o
829 f heterogeneous traffic flows on ship traffic efficiency: A prediction and simulation ap
830 proach. *Ocean Engineering*, 294, 116660, <https://doi.org/10.1016/j.oceaneng.2023.116660>.

831 Liu, J., Zhou, F., Wang, M., 2010. Simulation of waterway traffic flow at harbor based o
832 n the ship behaviour and cellular automata. In: *Proceedings of International Conferenc
833 e on Artificial Intelligence and Computational Intelligence*, pp. 542–546, [https://doi.org/
834 /10.1109/AICI.2010.352](https://doi.org/10.1109/AICI.2010.352).

835 Liu, J., Liu, Y., Qi L., 2021. Modelling liquefied natural gas ship traffic in port based on cellular
836 automaton and multi-agent system. *The Journal of Navigation*, 2021, 74(3), 533-548,
837 <https://doi.org/10.1017/S0373463321000059>.

838 Liu, R., He, D., Wang, L., Xu, H., 2014. Ant Colony Optimization Applied to the Three Gorges
839 Ship Lock Arrangement Optimization. *Applied Mechanics and Materials*, 543, 1663-1666,
840 10.4028/www.scientific.net/AMM.543-547.1663.

841 Małecki, K., 2018. A computer simulation of traffic flow with on-street parking and drivers’
842 behaviour based on cellular automata and a multi-agent system. *Journal of computational
843 science*, 28, 32-42, <https://doi.org/10.1016/j.jocs.2018.07.005>.

844 Mavrikakis, D., Kontinakis, N., 2008. A queueing model of maritime traffic in Bosphorus Straits.
845 *Simulation Modelling Practice and Theory*, 16(3), 315-328,
846 <https://doi.org/10.1016/j.simpat.2007.11.013>

847 Montewka, J., Ehlers, S., Goerlandt, F., Hinz, T., Tabri, K., Kujala, P., 2014. A framework
848 for risk assessment for maritime transportation systems - A case study for open sea
849 collisions involving Ro Pax vessels. *Reliability Engineering and System Safety*, 124,14
850 2-157, <https://doi.org/10.1016/j.ress.2013.11.014>.

851 Muirhead, J. R., Minton, M. S., Miller, W. A., Ruiz, G. M., 2015. Projected effects of th
852 e Panama Canal expansion on shipping traffic and biological invasions. *Diversity and
853 Distributions*, 21(1), 75-87, <https://doi.org/10.1111/ddi.12260>.

854 Nagel, K., Schreckenberg, M., 1992. A cellular automaton model for freeway traffic. *Journal De
855 Physique I*, 2, 2221–2229, <https://doi.org/10.1051/jp1:1992277>.

856 Nofandi, F., Widyaningsih, U., Rakhman, R. A., Mirianto, A., Zuhri, Z., Harini, N. V., 2022,
857 September. Case Study of Ship Traffic Crowds in The Malacca Strait-Singapore by Using
858 Vessel Traffic System. In *IOP Conference Series: Earth and Environmental Science (Vol. 1081,*

859 No. 1, p. 012009), IOP Publishing. DOI 10.1088/1755-1315/1081/1/012009.

860 Pagano, A., Wang, G., Sánchez, O., Ungo, R., Tapiero, E., 2016. The impact of the Panama Canal
861 expansion on Panama's maritime cluster. *Maritime Policy & Management*, 43(2), 164-178,
862 <https://doi.org/10.1080/03088839.2016.1140241>.

863 Qi, L., Zheng, Z., Gang, L., 2017a. Marine traffic model based on cellular automaton: con-
864 sidering the change of the ship's velocity under the influence of the weather and sea.
865 *Physica A: Statistical Mechanics and its Applications*, 480-494, [https://doi.org/10.1016](https://doi.org/10.1016/j.physa.2017.04.125)
866 [/j.physa.2017.04.125](https://doi.org/10.1016/j.physa.2017.04.125).

867 Qi, L., Zheng, Z., & Gang, L. 2017b. A cellular automaton model for ship traffic flow in
868 waterways. *Physica A: Statistical Mechanics and its Applications*, 471, 705-717, [http](http://doi.org/10.1016/j.physa.2016.12.028)
869 [s://doi.org/10.1016/j.physa.2016.12.028](http://doi.org/10.1016/j.physa.2016.12.028).

870 Qi, L., Ji, Y., Balling, R., Xu, W., 2021. A cellular automaton-based model of ship traffic
871 flow in busy waterways. *The Journal of Navigation*, 2021, 74(3), 605-618, [https://doi.](https://doi.org/10.1017/S0373463320000636)
872 [org/10.1017/S0373463320000636](https://doi.org/10.1017/S0373463320000636).

873 Qu, X., Meng, Q., 2012a. The economic importance of the Straits of Malacca and Singap-
874 ore: An extreme-scenario analysis. *Transportation Research Part E: Logistics and Trans-*
875 *portation Review*, 48(1), 258-265, <https://doi.org/10.1016/j.tre.2011.08.005>

876 Qu, X., Meng, Q., 2012b. Development and applications of a simulation model for vessels
877 in the Singapore Straits. *Expert Systems with Applications*, 39(9), 8430-8438, [https://](https://doi.org/10.1016/j.eswa.2012.01.176)
878 doi.org/10.1016/j.eswa.2012.01.176.

879 Rahimikelarijani, B., Abedi, A., Hamidi, M., Cho, J., 2018. Simulation modeling of Houst
880 on Ship Channel vessel traffic for optimal closure scheduling. *Simulation Modelling P*
881 *ractice and Theory*, 80, 89-103, <https://doi.org/10.1016/j.simpat.2017.10.004>.

882 Ren, G., Jiang, H., Chen, J., Huang, Z., Lu, L., 2016. Heterogeneous cellular automata model for
883 straight-through bicycle traffic at signalized intersection. *Physica A: Statistical Mechanics and*
884 *its Applications*, 451, 70-83, <https://doi.org/10.1016/j.physa.2015.12.159>.

885 Ruan, X., Zhou, J., Tu, H., Jin, Z., Shi, X., 2017. An improved cellular automaton with axis
886 information for microscopic traffic simulation. *Transportation Research Part C: Emerging*
887 *Technologies*, 78, 63-77, <https://doi.org/10.1016/j.trc.2017.02.023>.

888 Shi, S., Zhang, D., Su, Y., Wan, C., Zhang, M., Liu, C., 2019. A fuzzy-based decision-making model
889 for improving the carrying capacity of ship locks: a three gorges dam case. *Journal of Marine*
890 *Science and Engineering*, 7(8), 244, <https://doi.org/10.3390/jmse7080244>.

891 Sun, Z., Chen, Z., Hu, H., Zheng, J., 2015. Ship interaction in narrow water channels: A two-lane
892 cellular automata approach. *Physica A: Statistical Mechanics and its Applications*, 431, 46-51,
893 <https://doi.org/10.1016/j.physa.2015.02.079>.

894 Sun, L., Cheng, Z., Kong, D., Xu, Y., Wen, S., Zhang, K., 2023. Modeling and analysis of human-
895 machine mixed traffic flow considering the influence of the trust level toward autonomous
896 vehicles. *Simulation Modelling Practice and Theory*, 125, 102741,
897 <https://doi.org/10.1016/j.simpat.2023.102741>.

898 Ungo, R., Sabonge, R., 2012. A competitive analysis of Panama Canal routes. *Maritime Policy &*
899 *Management*, 39(6), 555-570, <https://doi.org/10.1080/03088839.2012.728727>.

900 Vaněk, O., Jakob, M., Hrstka, O., Pěchouček, M., 2011. Using multi-agent simulation to improve
901 the security of maritime transit. In *International Workshop on Multi-Agent Systems and Agent-*
902 *Based Simulation* (pp. 44-58), Springer, Berlin, Heidelberg.

903 Vaněk, O., Jakob, M., Hrstka, O., Pěchouček, M., 2013. Agent-based model of maritime traffic in
904 piracy-affected waters. *Transportation Research Part C: Emerging Technologies*, 36, 157-176,
905 [doi:10.1016/j.trc.2013.08.009](https://doi.org/10.1016/j.trc.2013.08.009).

906 Vranken, T., Sliwa, B., Wietfeld, C., Schreckenberg, M., 2021. Adapting a cellular automata model

907 to describe heterogeneous traffic with human-driven, automated, and communicating
908 automated vehicles. *Physica A: Statistical Mechanics and its Applications*, 570, 125792,
909 <https://doi.org/10.1016/j.physa.2021.125792>.

910 Wang, J., Lv, W., Jiang, Y., Qin, S., Li, J., 2021. A multi-agent based cellular automata model for
911 intersection traffic control simulation. *Physica A: Statistical Mechanics and Its Applications*,
912 584, 126356, <https://doi.org/10.1016/j.physa.2021.126356>.

913 Wang, S. L., Schonfeld, P., 2007. Demand elasticity and benefit measurement in a waterway
914 simulation model. *Transportation research record*, 2033(1), 53-61. <https://doi.org/10.3141/2033-08>.

916 Wolfram, S., 1983. Statistical mechanics of cellular automata. *Reviews of modern physics*, 55(3),
917 601, <https://doi.org/10.1103/RevModPhys.55.601>.

918 Wolfram, S., 1984a. Cellular automata as models of complexity. *Nature*, 311(5985), 419-424,
919 <https://doi.org/10.1038/311419a0>.

920 Wolfram, S., 1984b. Universality and complexity in cellular automata. *Physica D: Nonlinear
921 Phenomena*, 10(1-2), 1-35, [https://doi.org/10.1016/0167-2789\(84\)90245-8](https://doi.org/10.1016/0167-2789(84)90245-8).

922 Yeldan, Ö., Colorni, A., Luè, A., Rodaro, E., 2012. A stochastic continuous cellular automata traffic
923 flow model with a multi-agent fuzzy system. *Procedia-Social and behavioural Sciences*, 54,
924 1350-1359, <https://doi.org/10.1016/j.sbspro.2012.09.849>.

925 Zhang, F., Li, J., & Zhao, Q., 2005. Single-lane traffic simulation with multi-agent system. In
926 *Proceedings. 2005 IEEE Intelligent Transportation Systems, 2005.* (pp. 56-60), IEEE.
927 10.1109/ITSC.2005.1520219.

928 Zhang, L., Meng, Q., Fwa, T. F., 2019. Big AIS data based spatial-temporal analyses of ship traffic
929 in Singapore port waters, *Transportation Research Part E: Logistics and Transportation
930 Review*, 129, 287-304. <https://doi.org/10.1016/j.tre.2017.07.011>.

931 Zhang, Y., Tian, H., Li, R., Liang, X., Li, J., 2022. Hybrid simulation model for navigation
932 performance evaluation of the Three Gorges–Gezhouba Dams under novel regulations.
933 *SIMULATION*, 00375497211072536, <https://doi.org/10.1177/00375497211072536>.

934 Zhang, X., Yuan, X., & Yuan, Y., 2008. Improved hybrid simulated annealing algorithm for
935 navigation scheduling for the two dams of the Three Gorges Project. *Computers &
936 Mathematics with Applications*, 56(1), 151-159, <https://doi.org/10.1016/j.camwa.2007.11.041>.

937 Zhao, H., Liu, X., Chen, X., Lu, J., 2018. Cellular automata model for traffic flow at intersections
938 in internet of vehicles. *Physica A: Statistical Mechanics and its Applications*, 494, 40-51,
939 <https://doi.org/10.1016/j.physa.2017.11.152>.

940 Zhao, X., Lin, Q., Yu, H., 2020. A co-scheduling problem of ship lift and ship lock at the Three
941 Gorges Dam. *IEEE Access*, 8, 132893-132910, 10.1109/ACCESS.2020.3009775.

942 Zhang, X., Li, R., Wang, C., Xue, B., Guo, W., 2024. Robust optimization for a class of ship traffic
943 scheduling problem with uncertain arrival and departure times. *Engineering Applications of
944 Artificial Intelligence*, 133, 108257, <https://doi.org/10.1016/j.engappai.2024.108257>.